

RECEIVED: January 5, 2024 REVISED: April 19, 2024 ACCEPTED: May 12, 2024 PUBLISHED: June 19, 2024

Multi-Higgs boson production with anomalous interactions at current and future proton colliders

Andreas Papaefstathiou $lue{\mathbb{D}}^a$ and Gilberto Tetlalmatzi-Xolocotzi $lue{\mathbb{D}}^{b,c}$

^aDepartment of Physics, Kennesaw State University, 830 Polytechnic Lane, Marietta, GA 30060, U.S.A.

E-mail: apapaefs@cern.ch, gtx@physik.uni-siegen.de

ABSTRACT: We investigate multi-Higgs boson production at proton colliders, in a framework involving anomalous interactions, focusing on triple Higgs boson production. We consider modifications to the Higgs boson self-couplings, to the Yukawa interactions, as well as new contact interactions of Higgs bosons with either quarks or gluons. To this end, we have developed a MadGraph5_aMC@NLO loop model, publicly available at [1], designed to incorporate the relevant operators in the production of multiple Higgs bosons (and beyond). We have performed cross section fits at various energies over the anomalous interactions, and have derived constraints on the most relevant anomalous coefficients, through detailed phenomenological analyses at proton-proton collision energies of 13.6 TeV and 100 TeV, employing the 6 b-jet final state.

Keywords: Anomalous Higgs Couplings, Higgs Properties, Higgs Production, SMEFT

ARXIV EPRINT: 2312.13562

^bLPNHE, Sorbonne Université, Paris Diderot Sorbonne Paris Cité, CNRS/IN2P3, Paris, France

^cTheoretische Physik 1, Center for Particle Physics Siegen (CPPS), Universität Siegen, Walter-Flex-Str. 3, 57068 Siegen, Germany

U	ontents	
1	Introduction	1
2	Phenomenological lagrangian	3
3	Monte Carlo event generation	4
	3.1 Loop × tree-level interference	4
	3.2 Higgs boson pair production	5
	3.3 Triple Higgs boson production	5
4	Phenomenology of triple Higgs boson production	6
	4.1 Cross section Fits	6
	4.2 Other constraints on anomalous couplings	8
	4.3 Statistical analysis	9
	4.4 Phenomenological analysis	11
	4.5 Results	16
5	Conclusions	16
A	D=6 effective field theory	17
В	The electroweak chiral lagrangian including a light Higgs boson	2 0
\mathbf{C}	Validation of the Monte Carlo implementation	22
D	Feynman diagrams	23
\mathbf{E}	Discovery and limits with up to three powers of anomalous operators	25
F	Cross section fits for triple and double Higgs boson production at various energies	26

1 Introduction

Measuring the interactions of the Higgs boson [2–6] with the rest of the Standard Model (SM), with itself (i.e. its self-interactions), and with potential new phenomena, is a crucial task for future collider experiments. There are multiple theoretical justifications for the importance of the Higgs field and how it interacts; for example, the Higgs doublet bilinear, $H^{\dagger}H$, is the only dimension-2 (D=2) singlet operator within the SM. This kind of operator readily allows for D=3 or D=4 interactions with one, or two, new scalar singlet fields, that may constitute part of a "hidden sector" of hitherto undetected particles. Therefore, the Higgs boson could be our primary window to this, potentially "dark", sector, that could comprise part, or all, of dark matter. Another reason of the importance of the Higgs boson's interactions is that

they may illuminate the mechanism of baryogenesis — in particular, if this process occurred during the electroweak phase transition, the period during which the Higgs field acquires a vacuum expectation value (VEV), then the Higgs field may be one of the protagonists of electroweak baryogenesis (see, e.g. [7–21]). A central rôle in this mechanism is played by the Higgs potential, which, within the SM, is introduced in a rather ad-hoc manner. The form of this potential can, at least in principle, be directly probed by measuring the Higgs boson's self-interactions through multi-Higgs boson production processes: the triple self-coupling can be probed through Higgs boson pair production, and the quartic through triple production.

Novel Higgs boson interactions, to new or to SM particles, may arise at the electroweak scale, but they may also appear at higher scales, $\mathcal{O}(\text{few TeV})$. If this is the case, we can parametrize our ignorance using a higher-dimensional effective field theory (EFT), see, e.g. [22– 24. Neglecting lepton-number violating operators, the lowest-dimensionality EFT that can be written down consists of D=6 operators. Upon electroweak symmetry breaking, the Higgs boson would acquire a VEV and these operators would result in several new interactions, as well modifications of the SM interactions of the Higgs boson. Several of the operators in the physical basis of the Higgs boson scalar (h) would then have coefficients that are correlated, according to D=6 EFT. These correlations, however, may be broken by even higher-dimensional operators (e.g. D=8), particularly if the new phenomena are closer to the electroweak scale. Therefore, it may be beneficial to lean towards a more agnostic, and hence more phenomenological, approach and, while still remaining inspired by D=6EFT, consider fully uncorrelated, "anomalous" interactions of the Higgs boson with the SM. These kind of interactions can also be achieved within the framework of the electroweak chiral Lagrangian including a light Higgs boson, where free coefficients for all Higgs couplings are obtained [25–35]. This framework provides a consistent EFT justification of the usual "\(\tilde{\epsilon}\) "formalism. The description of the Higgs boson's interactions in terms of uncorrelated coefficients is the approach that we pursue here.

Within the realm of self-coupling measurements, and beyond, Higgs boson pair production has received considerable attention from both the experimental (e.g. [36–65]) and theoretical (e.g. [66-124]) point of view, particularly following the discovery of the Higgs boson. Owing to its much smaller SM cross section at hadron colliders [90], triple Higgs boson has understandably received much less attention. To the extent of our knowledge, it was first investigated in [125], where it was demonstrated that the prospects for the measurement of the quartic self-coupling will be very challenging, both at the LHC and a future 'VLHC' at a center-of-mass energy of 200 TeV. Subsequent studies of triple Higgs boson production at future colliders [126–135], with the knowledge of the value of the Higgs boson mass, and the prospects for Higgs boson pair production measurements at hand, further quantified the difficulty of this measurement, nevertheless demonstrating that some useful information may be obtained via the process. The situation at LHC energies is much more dire, as expected, requiring either new phenomena for sufficient enhancement [136], or very large new contributions to the Higgs boson's self-interactions [137]. Up to now, all of the phenomenological studies addressing triple Higgs boson production, apart from discussions of the cross section modifications in an EFT in [138], have considered only the effects of modifications of the self-couplings. However, due to their loop-induced nature,

proceeding via heavy quark loops, multi-Higgs boson production processes are highly sensitive to modifications of the heavy quark Yukawa couplings, as well as to additional quark- or gluon-Higgs boson contact interactions that generically arise in EFTs. Such effects have been studied within the context of Higgs boson pair production, see, e.g. [139, 140]. In the present article we study, for the first time to the best of our knowledge, the combined effect of modifications to the self-couplings, Yukawa interactions, and new heavy-quark- or gluon-Higgs boson contact interactions in triple Higgs boson production, within the aforementioned EFT-inspired anomalous coupling picture. To achieve this, we have constructed a specialized anomalous-coupling model within the MadGraph5_aMC@NLO event generator that incorporates the full interference effects between contributing diagrams.

The paper is organized as follows: in section 2 we introduce the phenomenological Lagrangian that we employ in our study, inspired by an EFT extension of the SM. In section 3 we discuss the details of the Monte Carlo implementation of the MadGraph5_aMC@NLO model, briefly addressing its usage for Higgs boson pair and triple production. In section 4 we discuss our phenomenological analysis of triple Higgs boson production, focusing on cross section fits, existing constraints on the anomalous couplings, and the extraction of limits on the most relevant coefficients through the 6 b-jet final state. We present our conclusions and outlook in section 5. In addition, in appendix A we describe the D=6 EFT Lagrangian relevant to Higgs boson production processes, i.e. the linear EFT approach, and in appendix B we discuss the nonlinear approach through the electroweak chiral Lagrangian. In appendix C we discuss aspects of the validation of the Monte Carlo model. In appendix D we discuss relevant Feynman diagrams that appear within our framework, up to two operator insertions. Finally, in appendix E we discuss limits obtained with up to three powers of anomalous operators (at the matrix element-squared level) instead of the two presented in the main text, and in appendix F we present supplementary cross section fits at various proton collision energies.

2 Phenomenological lagrangian

To allow for additional freedom, we have modified the D=6 EFT Lagrangian relevant to Higgs boson processes, derived in detail in appendix A (eq. (A.11)), breaking the correlations between several of the interactions that originate in the D=6 EFT. This yields more flexibility when exploring multi-Higgs boson production experimentally. Nevertheless, D=6 EFT can be trivially restored by reinstating the appropriate relations between the coefficients (see below). We also provide additional EFT justification for this approach, inspired by the electroweak chiral Lagrangian including a light Higgs boson in appendix B.

To achieve this, we have defined new anomalous couplings d_3 and d_4 , as modifications of the triple and quartic self-couplings, c_{g1} and c_{g2} as interactions of two gluons and one or two Higgs bosons, respectively, and c_{f1} , c_{f2} and c_{f3} as interactions between fermion-antifermion pairs, and one, two or three Higgs bosons, respectively, leading to the following

phenomenological Lagrangian:

$$\mathcal{L}_{\text{Pheno}} = -\frac{m_h^2}{2v} \left(1 + d_3 \right) h^3 - \frac{m_h^2}{8v^2} \left(1 + d_4 \right) h^4
+ \frac{\alpha_s}{4\pi} \left(c_{g1} \frac{h}{v} + c_{g2} \frac{h^2}{2v^2} \right) G_{\mu\nu}^a G_a^{\mu\nu}
- \left[\frac{m_t}{v} \left(1 + c_{t1} \right) \bar{t}_L t_R h + \frac{m_b}{v} \left(1 + c_{b1} \right) \bar{b}_L b_R h + \text{h.c.} \right]
- \left[\frac{m_t}{v^2} \left(\frac{3c_{t2}}{2} \right) \bar{t}_L t_R h^2 + \frac{m_b}{v^2} \left(\frac{3c_{b2}}{2} \right) \bar{b}_L b_R h^2 + \text{h.c.} \right]
- \left[\frac{m_t}{v^3} \left(\frac{c_{t3}}{2} \right) \bar{t}_L t_R h^3 + \frac{m_b}{v^3} \left(\frac{c_{b3}}{2} \right) \bar{b}_L b_R h^3 + \text{h.c.} \right].$$
(2.1)

To recover the D=6 EFT Lagrangian relevant to the Higgs sector (i.e. eq. (A.11)), one would need to simply set: $d_3=c_6$, $d_4=6c_6$, $c_{g1}=c_{g2}$, $c_{f1}=c_{f2}=c_{f3}$.

The implementation of this study further modifies the above phenomenological Lagrangian to match more closely the LHC experimental collaboration definitions:

$$\mathcal{L}_{\text{PhenoExp}} = -\lambda_{\text{SM}} v \left(1 + d_{3}\right) h^{3} - \frac{\lambda_{\text{SM}}}{4} \left(1 + d_{4}\right) h^{4}
+ \frac{\alpha_{s}}{12\pi} \left(c_{g1} \frac{h}{v} - c_{g2} \frac{h^{2}}{2v^{2}}\right) G_{\mu\nu}^{a} G_{a}^{\mu\nu}
- \left[\frac{m_{t}}{v} \left(1 + c_{t1}\right) \bar{t}_{L} t_{R} h + \frac{m_{b}}{v} \left(1 + c_{b1}\right) \bar{b}_{L} b_{R} h + \text{h.c.}\right]
- \left[\frac{m_{t}}{v^{2}} c_{t2} \bar{t}_{L} t_{R} h^{2} + \frac{m_{b}}{v^{2}} c_{b2} \bar{b}_{L} b_{R} h^{2} + \text{h.c.}\right]
- \left[\frac{m_{t}}{v^{3}} \left(\frac{c_{t3}}{2}\right) \bar{t}_{L} t_{R} h^{3} + \frac{m_{b}}{v^{3}} \left(\frac{c_{b3}}{2}\right) \bar{b}_{L} b_{R} h^{3} + \text{h.c.}\right],$$
(2.2)

where we have taken $\lambda_{\rm SM} \equiv m_h^2/2v^2$.

The CMS parametrization is then obtained by setting: $\kappa_{\lambda} = (1 + d_3)$, $k_t = c_{t1}$, $c_2 = c_{t2}$, $c_g = c_{g1}$, $c_{gg} = c_{2g}$ and the ATLAS parametrization by $c_{hhh} = (1 + d_3)$, $c_{ggh} = 2c_{g1}/3$, $c_{gghh} = -c_{g2}/3$. The Lagrangian of eq. (2.2) encapsulates the form of the interactions that we employ for the rest of our phenomenological analysis.

3 Monte Carlo event generation

3.1 Loop \times tree-level interference

The implementation of the Lagrangian of eq. (2.2) in MadGraph5_aMC@NLO (MG5_aMC) [141, 142] follows closely the instructions for proposed code modifications found in [143]. These modifications essentially introduce tree-level diagrams in the form of "UV counter-terms", that are generated along with any loop-level diagrams, allowing the calculation of interference terms between them. The model of the present article, created through this procedure, has been fully validated by direct comparison to an implementation of Higgs boson pair production in D=6 EFT in the HERWIG 7 Monte Carlo, and by taking the limit of a heavy scalar boson for those vertices that do not appear in that process. See appendix C for further

¹As suggested by Valentin Hirschi.

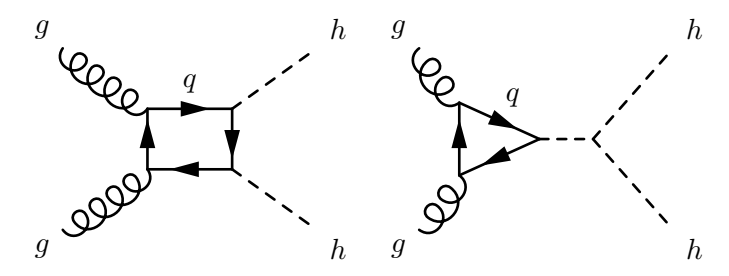


Figure 1. Example Feynman diagrams for leading-order gluon-fusion Higgs boson pair production in the Standard Model.

details of the latter effort. The necessary modifications to the MG5_aMC codebase,² as well as the model can be found in the public gitlab repository at [1].³

3.2 Higgs boson pair production

Higgs boson pair production contains a subset of all diagrams relevant to triple Higgs boson production, minus one Higgs boson insertion, and therefore we begin by investigating this process, so as to provide a simple example.

MG5_aMC allows for calculation of the interference terms via one insertion of the operator at the squared matrix-element level $(|\mathcal{M}|^2)$:

generate g g > h h [noborn=MHEFT QCD] MHEFT^2<=1</pre>

i.e. schematically: $|\mathcal{M}|^2 \sim \bullet 1 + \bullet c_i$. The classes of diagrams that are included in addition to the SM ones (figure 1), are those that appear in figure 8, found in appendix D.

Alternatively, one can obtain: the interference terms of one or two insertions with the SM, and the squares of one-insertion terms (equivalent to two powers of the anomalous couplings) via:

generate g g > h h [noborn=MHEFT QCD] MHEFT^2<=2</pre>

where schematically this would correspond to $|\mathcal{M}|^2 \sim \bullet 1 + \bullet c_i + \star c_i c_j$. The classes of diagrams of figure 9 (appendix D) appear in addition.

3.3 Triple Higgs boson production

For the investigation of triple Higgs boson production, which constitutes the focus of this article, we included the interference terms of one or two insertions with the SM and the squares of one-insertion terms through:

generate g g > h h h [noborn=MHEFT QCD] MHEFT^2<=2</pre>

The results with up to three powers of the anomalous operators, more appropriate within the framework of the electroweak chiral Lagrangian (appendix B), are presented in appendix E.

²At present available for versions 2.9.15 and 3.5.0.

³It is interesting to note here that there exists a more comprehensive MG5_aMC treatment of one-loop computations in the standard-model effective field theory at D = 6 (dubbed "smeft@nlo") [138], which should directly map to the D = 6 limit of the present article.

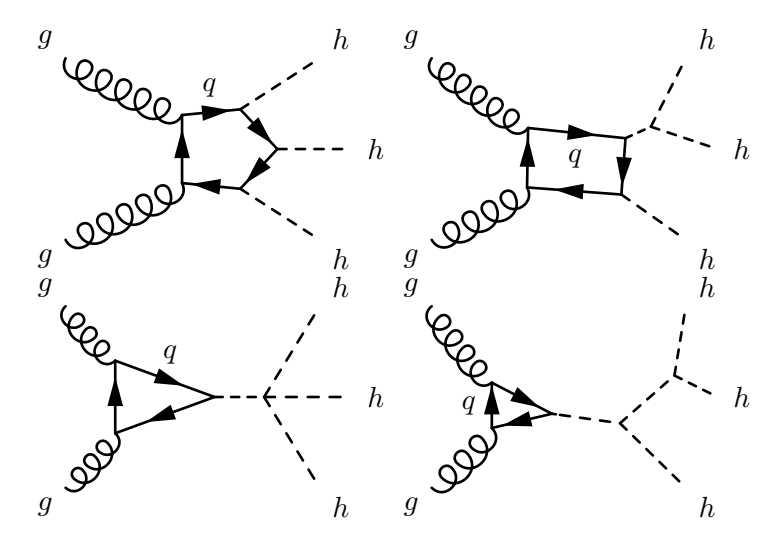


Figure 2. Example Feynman diagrams for leading-order gluon-fusion Higgs boson triple production in the Standard Model.

- 55	1	d_3	d_4	c_{q1}	c_{q2}	c_{t1}	c_{t2}	c_{t3}	c_{b1}	c_{b2}	c_{b3}
c_{b3}	0.161	-0.0809	-0.00396	-0.0182	0.124	0.598	-0.474	-0.0434	-0.0189	0.0109	0.00719
c_{b2}	0.106	-0.0752	0.00692	-0.00740	0.0949	0.433	-0.509	0.162	-0.0219	0.00489	
c_{b1}	-0.125	0.177	-0.0457	-0.00903	-0.166	-0.675	1.38	-0.941	0.0317		
c_{t3}	-2.72	-1.57	1.33	0.906	-0.316	-4.64	-18.2	13.0			
c_{t2}	-3.61	4.05	-0.872	-0.0482	-4.15	-17.6	15.3				
c_{t1}	6.94	-3.17	-0.309	-0.850	5.16	12.6					
c_{g2}	1.39	-0.704	-0.0312	-0.156	0.538						
c_{g1}	-0.278	0.0426	0.0484	0.0256							
d_4	-0.158	-0.0703	0.0340								
d_3	-0.750	0.292									

Table 1. Polynomial coefficients, A_i (second column only) and B_{ij} , relevant for the determination of the cross section for leading-order Higgs boson triple production, in the form $\sigma/\sigma_{\rm SM}-1=\sum_i A_i c_i+\sum_{i,j} B_{ij} c_i c_j$, where $c_i \in \{d_3, c_{g1}, c_{g2}, c_{t1}, c_{t2}, c_{b1}, c_{b2}, \}$, at $E_{\rm CM}=13.6$ TeV.

As in the case of Higgs boson pair production, our current treatment would schematically correspond to $|\mathcal{M}|^2 \sim \bullet 1 + \bullet c_i + \star c_i c_j$. The classes of the various diagrams that appear are shown in figure 2 for the SM, and in figures 10 for one insertion, and 11 for two insertions, in appendix D.⁴

4 Phenomenology of triple Higgs boson production

4.1 Cross section Fits

By employing our Monte Carlo implementation of eq. (2.2), We have performed cross section fits at a proton-proton collider at 13, 13.6, 14, 27, and 100 TeV, over all coefficients relevant to either Higgs boson pair or triple production. Two-dimensional projections of the fits for $E_{\rm CM}=13.6$ TeV appear in figure 3 for triple production. In this figure, for each corresponding plot, all other coefficients have been set to zero, for the sake of simplicity.

⁴We note here that a different number of insertions can be achieved by modifying the MHEFT^2<= part of the command. The maximum number of possible insertions depends on the process considered.

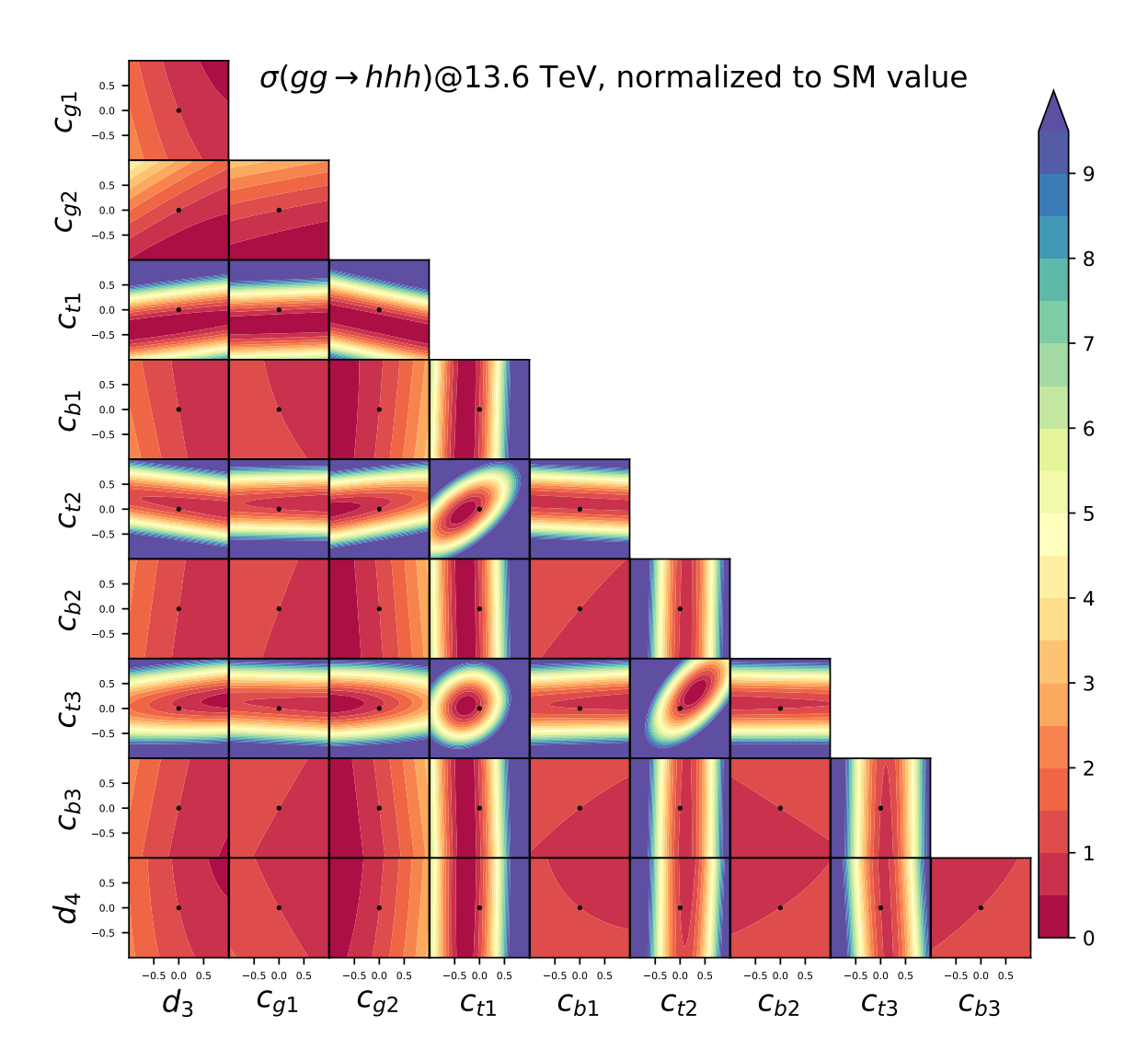


Figure 3. Fit of the cross section for triple Higgs boson production at 13.6 TeV, normalized to the SM value. For each combination of couplings, the other couplings have been set to zero for simplicity. Each change of color in the contours represents a shift of a factor of $0.5 \times$ the SM value.

The numerical values of the polynomial coefficients, yielding the cross section in the form $\sigma/\sigma_{\rm SM}-1=\sum_i A_i c_i+\sum_{i,j} B_{ij} c_i c_j$, where $c_i\in\{d_3,d_4,c_{g1},c_{g2},c_{t1},c_{t2},c_{t3},c_{b1},c_{b2},c_{b3}\}$, are shown for $E_{\rm CM}=13.6$ TeV in table 1 for triple production. For Higgs boson pair production at $E_{\rm CM}=13.6$ TeV, see table 9, in appendix F. The coefficients for both processes, at $E_{\rm CM}=13$, 14, 27 and 100 TeV can be found in appendix F. The table should be read as follows: each value shown corresponds to the coefficient multiplying the product of the couplings of the corresponding first column and last row, respectively. As an example, with reference to table 1, the coefficient of the term proportional to d_4d_3 is -0.0703, i.e. read off the second row, third column. Using these coefficients, one can construct the cross section for any given value of the anomalous couplings.

All the fits for the signal processes, and subsequent simulations, have been performed using the MSHT20nlo_as118 PDF set [144] and the default dynamical scale choice (option 3) in MG5 aMC, which corresponds to the sum of the transverse mass divided by 2.

	Percentage uncertainties								
	HL-LHC	FCC-hh	Ref.						
$\delta(d_3)$	50	5	[145] (table 12)						
$\delta(c_{g1})$	2.3	0.49	[145] (table 3)						
$\delta(c_{g2})$	5	1	[140] (figure 12, right)						
$\delta(c_{t1})$	3.3	1.0	[145] (table 3)						
$\delta(c_{t2})$	30	10	[140] (figure 12, right)						
$\delta(c_{b1})$	3.6	0.43	[145] (table 3)						
$\delta(c_{b2})$	30	10	assumed same as c_{t2}						

Table 2. Estimates of percentage uncertainties (%) obtained on the subset of anomalous couplings that appear in other processes at the HL-LHC and FCC-hh. The last column provides the source for these numbers.

We note here that the expected contribution of bottom-quark loops in the SM, both at LHC energies and at 100 TeV, is expected to be $\mathcal{O}(0.1\%)$. Therefore, anomalous couplings of the Higgs boson to the bottom quark are included merely for completeness, and furthermore, this ensures that we can safely neglect charm quark contributions in our analysis.

4.2 Other constraints on anomalous couplings

The majority of the anomalous couplings that appear in the phenomenological Lagrangian of eq. (2.2) are already tightly constrained by other processes that involve the interactions of gluons, top and bottom quarks with the Higgs boson. The two exceptions that are not presently constrained are the anomalous interactions of three Higgs bosons and two top or bottom quarks, with relevant coefficients c_{t3} and c_{b3} , as well as the anomalous modification to the Higgs boson's quartic interaction, related to the d_4 coefficient. While it is beyond the scope of the present study to perform a full fit, involving several processes and constraints, with their associated correlations, it is important to provide order-of-magnitude estimates for the two scenarios that we examine: the 13.6 TeV high-luminosity LHC, and the 100 TeV FCC-hh at the end of its lifetime.

We consider the constraints on c_{t1} , c_{b1} and c_{g1} that would arise within the "kappa-0" scenario, as they are defined in [145] (table 3). For the HL-LHC we consider those labeled "HL-LHC", and for the 100 TeV FCC-hh, we consider those projected after the combined results of "FCC-ee240+FCC-ee365", "FCC-eh", and "FCC-hh" for the FCC-hh, collectively labeled "FCC-ee/eh/hh". For the modifications to the Higgs boson triple self-coupling, we use the values quoted for the "di-Higgs exclusive" results for the "HL-LHC", shown in table 12 of [145]. For c_{g2} and c_{t2} , we assume approximate constraints derived from the results of the analysis of [140]. Due to the lack of concrete studies in the literature for c_{b2} , to the best of our knowledge, we have assumed that the constraint is identical to that of c_{t2} , obtained from [140]. For all the coefficients, we assume that the central value of these future measurements will be at zero. The assumed constraints are summarized as percentage uncertainties in table 2, along with the corresponding references, for convenience.

4.3 Statistical analysis

The goal of the present phenomenological analysis is two-fold: on the one hand, we wish to determine if triple Higgs boson production itself can be observed at the end of the HL-LHC or FCC-hh lifetime, and on the other, we wish to calculate the constraints that would be obtained on the anomalous couplings, given the assumption the SM is the true underlying theory. The first goal corresponds to the null hypothesis being the absence of triple Higgs boson production, whereas the latter corresponds to the null hypothesis being SM triple Higgs boson production, i.e. triple production with all the anomalous coupling coefficients set to zero.

For the first of these goals, i.e. to determine the significance, Σ , of observing triple Higgs boson production for a certain anomalous coupling parameter-space point, we optimize the signal versus background discrimination according to our phenomenological analysis (described in the following section, 4.4), to obtain the maximum significance over the set of cuts for SM triple Higgs boson production. Since we expect the number of signal events to be much lower than that for the background, we employ the following formula for the significance:

$$\Sigma = \frac{S}{\sqrt{B + (\alpha B)^2}} \,, \tag{4.1}$$

where S and B are the expected number of signal and background events, respectively, at a given integrated luminosity \mathcal{L} , and α is a factor that we employ to model the systematic uncertainty present in the background estimation. During our search for the maximum SM triple Higgs boson production significance, we used the value $\alpha = 0$, i.e. we optimized the quantity S/\sqrt{B} . Subsequently, all results are presented with this optimal set of cuts, obtained separately for each collider, while setting the systematic uncertainty factor $\alpha = 0.05$.

We have derived the expected "evidence" (3σ) and "discovery" (5σ) limits on the observation of triple Higgs boson production on the (c_{t3}, d_4) -plane, where the novel information coming from triple Higgs boson production is expected to arise. Furthermore, we have derived the 68% confidence level (C.L.) (1σ) and 95% C.L. (2σ) expected limits on the same plane, given that the SM hypothesis is true (i.e. SM triple Higgs boson production). While doing so, we allow the coefficients d_3 and c_{t2} to vary. These will be constrained primarily via Higgs boson pair production, and since this is a challenging process in itself, will not be substantially constrained compared to the gluon-Higgs anomalous interactions, or the top-anti-top-Higgs anomalous coupling, c_{t1} , see table 2 for a quantification of this statement. In addition, we do not expect triple Higgs boson production to be competitive to Higgs boson pair production in terms of constraints on d_3 and c_{t2} , so we "marginalize" over these two. Note that, due to the fact that we are assuming minimal flavour violation, as discussed in appendix A, as well as for the sake of simplicity, we do not expect the effect of the c_{b3} coefficient to be as significant as that of c_{t3} , and therefore we have set c_{b3} to zero in the phenomenological analysis.

To derive the evidence and discovery limits for triple Higgs boson production, we assume that the number of signal and background events follow gaussian distributions, and define the uncertainty on the background number of events as:

$$\delta_{\rm B} = \sqrt{B + (\alpha B)^2} \ . \tag{4.2}$$

Then, the probability value (p-value) to obtain a given number of signal events, $S(\{c_i\})$, corresponding to the set of anomalous coupling coefficients $\{c_i\}$, is given by:

$$P(\{c_i\}) = \frac{1}{\sqrt{2\pi}\delta_{\rm B}} \exp\left[-\frac{S(\{c_i\})^2}{2\delta_{\rm B}^2}\right].$$
 (4.3)

To take into account the approximate constraints of table 2, that would be present, ignoring possible correlations that will exist between constraints, we multiply the p-values by a gaussian prior factor:

$$P_C(c_i) = \frac{1}{\sqrt{2\pi}\delta(c_i)} \exp\left[-\frac{c_i^2}{2\delta(c_i)^2}\right], \qquad (4.4)$$

at a value c_i of each of the anomalous coefficients d_3 and c_{t2} . We then marginalize by integrating over the d_3 and c_{t2} directions. Since this is done over a grid, the integral is represented by a sum over the grid points:

$$P_M(c_{t3}, d_4) = \sum_{(d_3, c_{t2})} \Delta d_3 \Delta c_{t2} P_C(d_3) P_C(c_{t2}) P(\{c_i\}) , \qquad (4.5)$$

where Δd_3 and Δc_{t2} are the bin widths in the d_3 and c_{t2} directions, respectively. The probability is then converted to χ^2 via the Python χ^2 inverse survival function for two degrees of freedom (scipy.stats.chi2.isf), and the 3σ and 5σ limits are found by drawing the iso-contours corresponding to $\chi^2 - \chi^2_{\min} = (11.8, 28.7)$, respectively. The results are shown in figure 4, in section 4.5.

For the determination of the constraints obtained for the null hypothesis being SM triple Higgs boson production, we follow a similar procedure. In this scenario, we assume that the number of events for both signal and background follow a gaussian distribution, as we did before, and hence the uncertainty on the number of total expected SM events is given by:

$$\delta_{\text{SM+B}} = \sqrt{S_{\text{SM}} + B + (\alpha B)^2} , \qquad (4.6)$$

where S_{SM} represents the expected number of events for SM triple Higgs boson production. Then the *p*-value to obtain a given number of events corresponding to an anomalous coupling parameter-space point, $S(\{c_i\})$, given that the SM is the truth, is given by:

$$\bar{P}(\{c_i\}) = \frac{1}{\sqrt{2\pi}\delta_{\text{SM+B}}} \exp\left[-\frac{(S_{\text{SM}} - S(\{c_i\}))^2}{2\delta_{\text{SM+B}}^2}\right] . \tag{4.7}$$

This p-value is then multiplied by the prior factors of eq. (4.4), and summed as before:

$$\bar{P}_M(c_{t3}, d_4) = \sum_{(d_3, c_{t2})} \Delta d_3 \Delta c_{t2} P_C(d_3) P_C(c_{t2}) \bar{P}(\{c_i\}) , \qquad (4.8)$$

followed by a conversion to the χ^2 value as before. The 68% (1 σ) and 95% (2 σ) confidence level (C.L.) intervals are found by drawing the iso-contours corresponding to $\chi^2 - \chi^2_{\min} = (2.28, 5.99)$, respectively. The results of this analysis are shown in figure 5, in section 4.5.

To obtain the one-dimensional limits on either of the d_4 or c_{t3} couplings alone, we take the procedure one step further: we sum over the additional marginalized coupling as in eq. (4.8), and convert the *p*-value into a χ^2 value. For the triple Higgs boson searches, we calculate the 3σ and 5σ evidence and discovery limits by finding the points that correspond to $\chi^2 - \chi^2_{\min} = (9.00, 25.0)$, respectively. For the expected constraints on the d_4 and c_{t3} coefficients, given that the SM is true, we calculate the 1σ and 2σ intervals by finding the points that correspond to $\chi^2 - \chi^2_{\min} = (0.99, 3.84)$, respectively. The results for the evidence and discovery points, and for the expected limits given that the SM is true, are shown in tables 5 and 6, respectively, in section 4.5.

In regard to the use of the Gaussian approximation in our analysis, we note here that, while the expected number of events for the case of the SM signal is low and, strictly speaking, Poisson statistics should be employed in that case, we would like to emphasize that this is not the case at the 1,2,3 and 5σ exclusion/discovery boundaries that we have deduced. To be concrete, for the HL-LHC case, to obtain a 1σ significance, we would need, given our estimates for the expected number of background events (table 4, top) B=419.6, the following number of signal events:

$$S \simeq 1 \times \sqrt{B + (\alpha B)^2} \simeq 29.32 \ . \tag{4.9}$$

For this expected number of signal events, the Gaussian approximation would yield a 68% confidence-level interval of 29.32 ± 5.41 , whereas the Poisson approximation would yield $29.32^{+4.48}_{-6.48}$. Given the other uncertainties that enter our phenomenological analysis, it is therefore reasonable to assume that events are Gaussian-distributed at the boundaries of the exclusion/discovery regions.

4.4 Phenomenological analysis

To obtain constraints on anomalous triple Higgs boson production at proton colliders, following the statistical procedure outlined above, we have performed a hadron-level phenomenological analysis of the 6 b-jet final-state originating from the decays of all three Higgs bosons to $b\bar{b}$ quark pairs. We closely follow the analysis of refs. [132, 136]. Parton-level events have been generated using the MG5_aMC anomalous couplings implementation constructed in the present article, with showering, hadronization, and simulation of the underlying event, performed via the general-purpose HERWIG 7 Monte Carlo event generator [146–153]. The event analysis was performed via the HwSim framework addon to HERWIG 7 [154]. No smearing due to the detector resolution or identification efficiencies have been applied to the final objects used in the analysis, apart from a b-jet identification efficiency, discussed below. We expect such effects to produce differences in binned jet observables of $\mathcal{O}(10\%)$ at the LHC, see for example [155, 156], and anticipate substantial improvement to this at the FCC-hh.

The branching ratio of $h \to bb$ will be modified primarily due to c_{t1} , c_{g1} , indirectly through modifications to the $h \to gg$ and $h \to \gamma\gamma$ branching ratios, and directly through c_{b1} . To take this effect into account, we employed the eHDECAY code [157]. The program eHDECAY includes QCD radiative corrections, and next-to-leading order electroweak corrections are only applied to the SM contributions. For further details, see ref. [157]. We have performed a fit of the eHDECAY branching ratio $h \to b\bar{b}$, and we have subsequently normalized this to the latest branching ratio provided by the Higgs Cross Section Working Group's Yellow Report [158, 159], BR $(h \to b\bar{b}) = 0.5824$. The fit is then used to rescale the final cross section

of $pp \to hhh \to (b\bar{b})(b\bar{b})(b\bar{b})$. The background processes containing Higgs bosons turned out to be subdominant with respect to the dominant QCD 6 *b*-jet and Z+jets backgrounds, and therefore we did not modify these when deriving the final cross sections.

For the generation of the backgrounds involving b-quarks not originating from either a Z or Higgs boson, we imposed the following generation-level cuts for the 100 TeV proton collider: $p_{T,b} > 30$ GeV, $|\eta_j| < 5.0$, and $\Delta R_{b,b} > 0.2$. The transverse momentum cut was lowered to $p_{T,b} > 20$ GeV for 13.6 TeV, except for the QCD 6 b-jet background, for which we produced the events inclusively, without any generation cuts.⁵ The selection analysis was optimized considering as a main backgrounds the QCD-induced process $pp \to (b\bar{b})(b\bar{b})(b\bar{b})$, and the Z+jets process (represented by $Z + (b\bar{b})(b\bar{b})$), which we found to be significant at LHC energies.

The event selection procedure for our analyses proceeds as follows: as in [132], an event is considered if it contains at least six b-tagged jets, of which only the six ones with the highest p_T are taken into account. A universal minimal threshold for the transverse momentum, $p_{T,b}$, of any of the selected b-tagged jets is imposed. In addition a universal cut on their maximum pseudo-rapidity, $|\eta_b|$, is also applied. We subsequently make use of the observable:

$$\chi^{2,(6)} = \sum_{qr \in I} (m_{qr} - m_h)^2 , \qquad (4.10)$$

where $I = \{jb_1jb_2, jb_3jb_4, jb_5jb_6\}$ is the set of all possible 15 pairings of 6-b tagged jets. Out of all the possible combinations we pick the one with the smallest value $\chi_{\min}^{2,(6)}$. The pairings of b-jets defining $\chi_{\min}^{2,(6)}$ constitute our best candidates for the reconstruction of the three Higgs bosons, h. Our studies have demonstrated that $\chi_{\min}^{2,(6)}$ is one of the most powerful observables to employ in signal versus background discrimination.

We further refine the discrimination power of the $\chi_{\min}^{2,(6)}$ variable by using the individual mass differences $\Delta m = |m_{qr} - m_h|$ in eq. (4.10), sorting them out according to $\Delta m_{\min} < \Delta m_{\text{med}} < \Delta m_{\text{max}}$, and imposing independent cuts on each of them. We also consider the transverse momentum $p_T(h^i)$ of each reconstructed Higgs boson candidate. These reconstructed particles are also sorted based on the value of $p_T(h^i)$, on which we then impose a cut. Besides the universal minimal threshold on $p_{T,b}$, introduced at the beginning of this section, we impose cuts on the three b-jets with the highest transverse momentum p_{T,b_i} , for i=1,2,3. The set of cuts $p_{T,b_3} < p_{T,b_2} < p_{T,b_1}$ is the second most powerful discriminating observable in our list. Finally, we also considered two additional geometrical observables. The first of them is the distance between b-jets in each reconstructed Higgs boson $\Delta R_{bb}(h^i)$. The second one is the distance between the reconstructed Higgs bosons $\Delta R(h^i, h^j)$ themselves.

Our optimization process then proceeds as in [132, 136]: we sequentially try different combination of cuts over the observables introduced above on our signal and background samples until we achieve a significance above 2 or when our number of Monte Carlo events is reduced so drastically that no meaningful statistical conclusions can be derived if this number becomes smaller (this happens for instance when for a given combination of cuts, we are left with less than 10 Monte Carlo events of signal or background).

⁵In general, the simulation of the QCD induced process $pp \to (b\bar{b})(b\bar{b})(b\bar{b})$ is one of the most challenging aspects of the phenomenological study. The samples are produced in parallel using OMNI cluster at the university of Siegen using the "gridpack" option available in MG5_aMC.

	Optimized cuts							
Observable	$13.6\mathrm{TeV}$	$100\mathrm{TeV}$						
$p_{T,b} >$	$25.95\mathrm{GeV}$	$35.00\mathrm{GeV}$						
$ \eta_b <$	2.3	3.3						
$\Delta R_{bb} >$	0.3	0.3						
$p_{T,b_i} >$	[25.95, 25.95, 25.95] GeV $i = 1, 2, 3$	$[170.00, 135.00, 35.00] \mathrm{GeV}$						
$\chi^{2,(6)} <$	$27.0\mathrm{GeV}$	$26.0\mathrm{GeV}$						
$\Delta m_{\rm min,med,max} <$	[100, 200, 300] GeV	[8, 8, 8] GeV						
$\Delta R_{bb}(h^i) <$	[3.5, 3.5, 3.5]	[3.5, 3.5, 3.5]						
$\Delta R(h^i, h^j) <$	[3.5, 3.5, 3.5]	[3.5, 3.5, 3.5]						
$p_T(h^i) >$	[0.0, 0.0, 0.0] GeV	[200.0, 190.0, 20.0] GeV						

Table 3. Optimized cuts determined for the phenomenological analysis. The indices i, j can take the values i, j = 1, 2, 3. For the cut $\Delta R(h^i, h^j)$ the three pairings correspond to (1, 2), (1, 3), (2, 3). The indexed elements should be read from left to right in increasing order. The last two rows refer to cuts over light jets.

For 100 TeV, the observables are optimized in the following order, (i) p_{Th} , (ii) $|\eta_b|$, (iii) $\chi^{2,(6)}$, (iv) Δm_{\min} , Δm_{med} , Δm_{\max} , (v) p_{T,b_1} and (vi) p_{T,b_2} . By testing different cut combinations over the variables above we reach a SM triple Higgs boson significance of $S/\sqrt{B} \simeq 2.33\sigma$ without b-jet tagging or $S/\sqrt{B} \simeq 1.43\sigma$ including the b-tagging factor (0.85). We note that this is an improvement over the previous result of [132], where the corresponding significance was around 1.7σ without b-tagging. For 13.6 TeV the optimization of the cuts follows a similar path, however after applying the cut on $\chi^{2,(6)}$ we are left with $\mathcal{O}(10)$ Monte Carlo events for background, and therefore the full procedure stops at a significance of only 0.23σ without b-jet tagging or 0.14σ with b-jet tagging (0.85). The concrete values of the cuts applied on the different kinematic variables depend on the center of mass energy of the collider under study, and are summarized on table 3. We note that the optimal set of cuts for the HL-LHC requires more central b-jets than that at the FCC-hh. The complete list of backgrounds, their initial cross sections, efficiency of cuts and expected number of events at each of the full collider luminosities, are given in table 4. It is interesting to note that the Z + (bb)(bb) is in fact the dominant one at the HL-LHC, whereas the reverse is true for the FCC-hh. It will be important to validate this result in a future detailed experimental study that consider the full effects of the detectors.

To employ the results of the SM analysis over the whole of the parameter space we are considering, we have performed a polynomial fit of the efficiency of the analysis on the signal, $\varepsilon_{\text{analysis}}(hhh)$, at various, randomly-chosen, combinations of anomalous coefficient values. In combination with the fits of the cross section, and the fit of the branching ratio of the Higgs boson to $(b\bar{b})$, we can estimate the number of events at a given luminosity, for a given collider for any parameter-space point within the anomalous coupling picture, which we dubbed $S(\{c_i\})$ in our discussion of the statistical approach we take, in section 4.3.

LHC Analysis (13.6 TeV)									
Process	$\sigma_{ m NLO}(6\ b{ m -jet})$ [fb]	$arepsilon_{ ext{analysis}}$	$N_{ m 3 imes10^3~fb^{-1}}^{ m cuts}$						
hhh(SM)	1.97×10^{-2}	0.12	2.77						
QCD $(b\bar{b})(b\bar{b})(b\bar{b})$	6136.12	1.00×10^{-5}	69.67						
$pp \to Z(b\bar{b})(b\bar{b})$	61.80	0.0045	318.17						
$pp \to ZZ(b\bar{b})$	2.16	0.0059	14.3						
$pp \to hZ(b\bar{b})$	0.45	0.0159	8.1						
$pp \to hhZ$	0.0374	0.034	1.45						
$pp \to hh(b\bar{b})$	0.0036	0.028	0.11						
LI $gg \to hZZ$	0.143	0.022	3.62						
LI $gg \to ZZZ$	0.124	0.013	1.76						
LI $gg \to hhZ$	0.0458	0.047	2.42						

	FCC-hh Analysis (100 TeV)									
Process	$\sigma_{ m NLO}(6\ b{ m -jet})$ [fb]	$arepsilon_{ m analysis}$	$N_{ m 20~ab^{-1}}^{ m cuts}$							
hhh(SM)	1.14	0.0115	98.90							
QCD $(b\bar{b})(b\bar{b})(b\bar{b})$	56.66×10^3	1.12×10^{-5}	4777.71							
$pp \to Z(b\bar{b})(b\bar{b})$	1285.37	3.04×10^{-5}	294.63							
$pp \to ZZ(b\bar{b})$	49.01	2.02×10^{-5}	7.48							
$pp \to hZ(b\bar{b})$	9.87	3.04×10^{-5}	2.26							
$pp \to hhZ$	0.601	5.95×10^{-4}	2.70							
$pp \to hh(b\bar{b})$	0.096	8.095×10^{-5}	« 1							
LI $gg \to hZZ$	8.28	1.62×10^{-4}	10.12							
LI $gg \to ZZZ$	6.63	4.05×10^{-5}	2.03							
LI $gg \to hhZ$	2.65	2.54×10^{-4}	5.07							

Table 4. The lists of processes considered during our phenomenological analysis, along with their respective cross sections to the 6 *b*-jet final state. The efficiencies $\varepsilon_{\rm analysis}$ and number of events $N_{\mathcal{L}}^{\rm cuts}$, correspond to those obtained after applying the set of cuts given in table 3. A *b*-jet identification efficiency of 0.85 (for each *b*-jet) has also been applied to obtain the number of events. For the HL-LHC we considered an integrated luminosity of $\mathcal{L} = 3000 \text{ fb}^{-1}$, and for the FCC-hh a luminosity of $\mathcal{L} = 20 \text{ ab}^{-1}$. To approximate higher-order corrections, a *K*-factor K = 2 has been included for all processes, with respect to the leading-order cross section. The background processes marked with "LI" represent loop-induced contributions that have been generated separately.

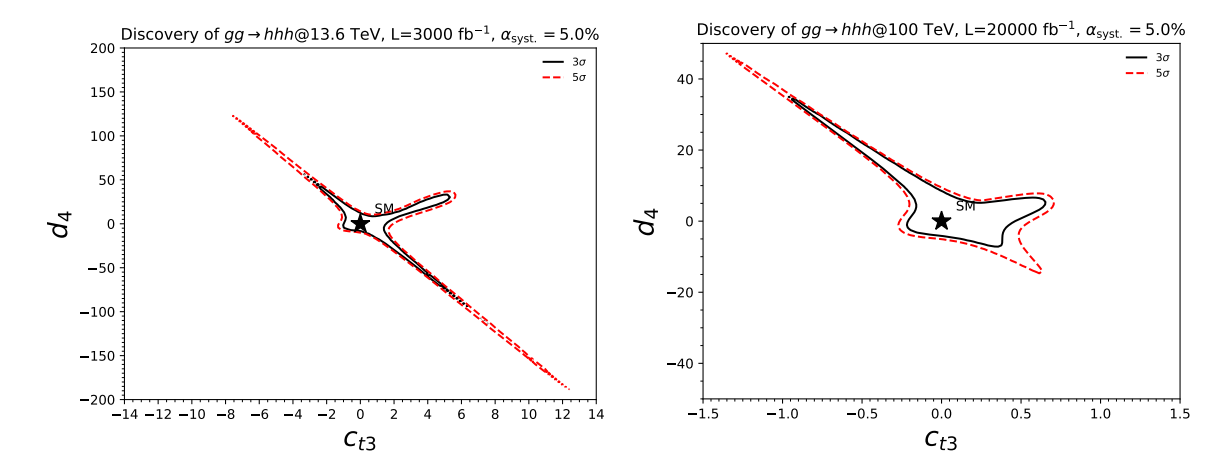


Figure 4. The 3σ evidence (black solid) and 5σ discovery (red dashed) curves on the (c_{t3}, d_4) -plane for triple Higgs boson production at $13 \text{ TeV}/3000 \text{ fb}^{-1}$ (left), and $100 \text{ TeV}/20 \text{ ab}^{-1}$ (right), marginalized over the c_{t2} and d_3 anomalous couplings. Note the differences in the axes ranges at each collider.

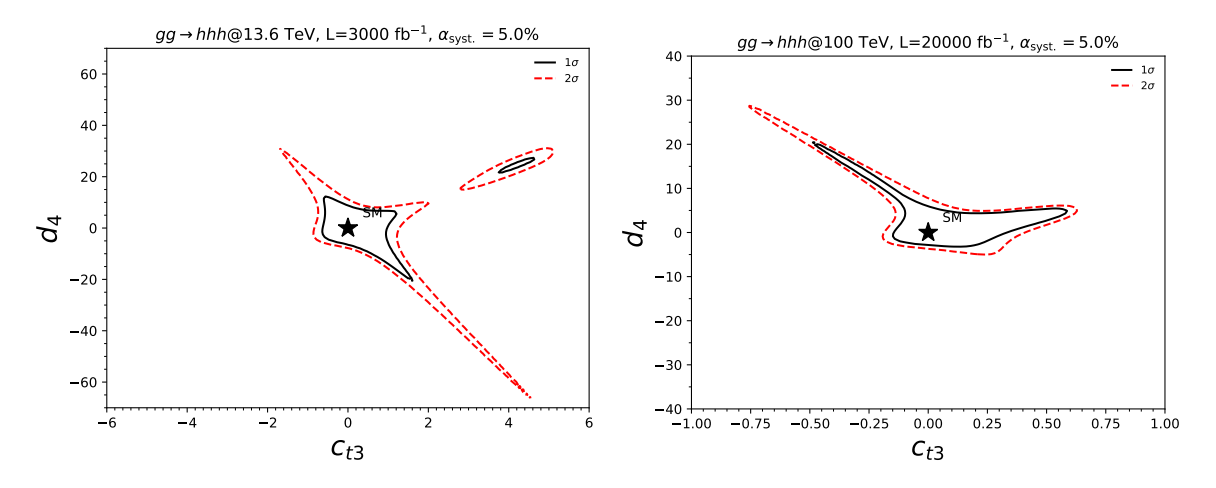


Figure 5. The 68% C.L. (1 σ , black solid) and 95% C.L (2 σ , red dashed) limit on the (c_{t3} , d_4)-plane for triple Higgs boson production at 13 TeV/3000 fb⁻¹ (left), and 100 TeV/20 ab⁻¹ (right), marginalized over the c_{t2} and d_3 anomalous couplings. Note the differences in the axes ranges at each collider.

	HL-LHC 3σ	HL-LHC 5σ	FCC-hh 3σ	FCC-hh 5σ
d_4	[-28.0, 41.7]	[-99.5, 152.9]	[-24.9, 20.8]	[-40.8, 23.1]
c_{t3}	[-2.1, 5.5]	[-7.1, 11.3]	[-0.8, 0.6]	[-1.2, 0.7]

Table 5. The 3σ evidence and 5σ discovery limits on for triple Higgs boson production, for the c_{t3} and d_4 coefficients at $13 \text{ TeV}/3000 \text{ fb}^{-1}$, and $100 \text{ TeV}/20 \text{ ab}^{-1}$, marginalized over c_{t2} , d_3 and either d_4 , or c_{t3} .

	HL-LHC 68%	HL-LHC 95%	FCC-hh 68%	FCC-hh 95%
d_4	[-6.6, 12.4]	[-10.0, 21.3]	[-3.9, 10.5]	[-10.6, 18.8]
c_{t3}	[-0.6, 1.1]	[-0.9, 3.6]	[-0.1, 0.3]	[-0.4, 0.6]

Table 6. The 68% C.L. (1σ) and 95% C.L (2σ) limits on c_{t3} and d_4 for triple Higgs boson production at 13 TeV/3000 fb⁻¹, and 100 TeV/20 ab⁻¹, marginalized over c_{t2} , d_3 and either d_4 , or c_{t3} .

4.5 Results

The main results of our two-dimensional analysis over the (c_{t3}, d_4) -plane are shown in figures 4 and 5. In particular, figure 4 shows the potential "evidence" and "discovery" regions (3σ and 5σ , respectively) for triple Higgs boson production at the high-luminosity LHC on the left $(13.6 \text{ TeV with } 3000 \text{ fb}^{-1} \text{ of integrated luminosity}), \text{ and at a FCC-hh} (100 \text{ TeV, with } 20 \text{ ab}^{-1})$ on the right. Evidently, very large modifications to the quartic self-coupling are necessary for discovery of triple Higgs boson production at the HL-LHC, ranging from $d_4 \sim 125$ for $c_{t3} \sim -8$, to $d_4 \sim \pm 40$ for $c_{t3} \sim 0$ and then down to $d_4 \sim -200$ for $c_{t3} \sim 12$. The situation is greatly improved, as expected, at the FCC-hh, where the range of d_4 is reduced to $d_4 \sim 40$ for $c_{t3} \sim -1.5$, and to $d_4 \sim -20$ for $c_{t3} \sim 1.0$. It is interesting to note that the whole of the parameter space with $c_{t3} \gtrsim 1.0$, or with $c_{t3} \lesssim -1.5$ is discoverable, at the FCC-hh at 5σ . For the potential 68% (1 σ) and 95% C.L. (2 σ) constraints of figure 5, the situation is slightly more encouraging for the HL-LHC, with the whole region of $d_4 \gtrsim 40$ or $d_4 \lesssim -60$ excluded at 95% C.L.. The corresponding region at 68% C.L. is $d_4 \gtrsim 20$ and $d_4 \lesssim -30$. For c_{t3} , it is evident that all the region $c_{t3} \lesssim -2$ and $c_{t3} \gtrsim 5$ will be excluded at 95% C.L. and $c_{t3} \lesssim -1$, $c_{t3} \gtrsim 4$ at 68% C.L.. On the other hand, the FCC-hh will almost be able to exclude the whole positive region of d_4 for any value of c_{t3} at 68% C.L.. This will potentially be achievable if combined with other Higgs boson triple production final states. For the c_{t3} coupling, both the constraints reach the $\mathcal{O}(\text{few }10\%)$ level for any value of d_4 .

The one-dimensional analysis' results, presented in tables 5 and 6, for the "evidence" and "discovery" potential, and exclusion limits, respectively, reflect the above conclusions. For instance, it is clear by examining table 5, that the HL-LHC will only see evidence of triple Higgs boson production in the 6 b-jet final state only if d_4 has modifications of $|d_4| \sim \mathcal{O}(\text{few } 10)$, and will only discover it if $|d_4| \sim \mathcal{O}(100)$. On the other hand, there could be evidence or discovery of Higgs boson triple production if $|c_{t3}| \sim \mathcal{O}(1-10)$. The 1σ and 2σ exclusion regions are much tighter, as expected, with $|d_4| \sim \mathcal{O}(10)$ at 1σ or 2σ at the HL-LHC, improving somewhat at the FCC-hh, and $|c_{t3}| \sim \mathcal{O}(0.1-1)$, both at the HL-LHC and FCC-hh.

5 Conclusions

We have conducted a phenomenological analysis of the triple Higgs boson production at the high-luminosity LHC (13.6 TeV with 3000 fb⁻¹) and a proposed future circular collider colliding protons at 100 TeV (20 ab⁻¹). For this analysis, we have constructed a model to be used with the MadGraph5_aMC@NLO event generator, which is publicly available at [1]. By examining the 6 b-jet final state, within a signal versus background analysis, we have concluded that interesting constraints can be obtained on the most relevant coefficients, d_4 and c_{t3} , representing modifications to the Higgs quartic self-coupling, and additional top-Higgs interactions, respectively. These are presented, for the HL-LHC and the FCC-hh, over the (c_{t3}, d_4) -plane in figures 4 and 5, showing the evidence/discovery potential of the triple Higgs boson production process itself, marginalized over the d_3 and c_{t2} coefficients, and the $1/2\sigma$ exclusion regions arising from the process on that plane. The one-dimensional evidence/discovery regions over either d_4 , or c_{t3} at both colliders are given in table 5, and the possible constraints extracted in table 6.

The results of our study demonstrate the importance of including additional contributions, beyond the modifications to the self-couplings, when examining multi-Higgs boson production processes, and in particular triple Higgs boson production. We are looking forward to a more detailed study for the HL-LHC, conducted by the ATLAS and CMS collaborations, including detector simulation effects, and the full correlation between other channels. From the phenomenological point of view, improvements will arise by including additional final states, e.g. targetting the process $pp \to hhh \to (b\bar{b})(b\bar{b})(\tau^+\tau^-)$, or by performing an analysis that leverages machine learning techniques to maximize significance. In summary, we believe that the triple Higgs boson production process should constitute part of a full multi-dimensional fit, within the anomalous couplings picture.

Acknowledgments

We extend our thanks to Alberto Tonero for his valuable early contributions to this project. A.P. acknowledges support by the National Science Foundation under Grant No. PHY 2210161. G.T.X. received support for this project from the European Union's Horizon 2020 research and innovation programme under the Marie Sklodowska-Curie grant agreement No 860881-HIDDeN [S.D.G.] and the Marie Sklodowska-Curie grant agreement No. 945422. This research was supported by the Deutsche Forschungsgemeinschaft (DFG, German Research Foundation) under grant 396021762 - TRR 257. We thank Wolfgang Kilian for interesting discussions. We would also like to thank the organizers of the HHH workshop that took place in July 2023 at the Inter University Center, in Dubrovnik, Croatia (IUC), for facilitating discussions on the subject matter presented here.

A D = 6 effective field theory

The phenomenological Lagrangian employed in this study can be motivated by considering the D=6 effective field theory (EFT) Lagrangian of ref. [139]. The discussion that follows has been adapted for the purposes of the present article.

New Physics associated to a new scale $\Lambda \gg v$ can be described in a model-independent way by augmenting the Lagrangian of the SM with all possible gauge-invariant operators of mass dimension D > 4, where the leading effects arise from D = 6 operators (neglecting lepton-number violating operators, irrelevant to our study). Working at this level, the

⁶This approach was taken in [137] at the HL-LHC for modifications of the Higgs boson's self-couplings.

extension of the SM that is relevant for multi-Higgs boson production reads:

$$\mathcal{L} = \mathcal{L}_{SM} + \frac{c_H}{2\Lambda^2} (\partial^{\mu} |H|^2)^2 - \frac{c_6}{\Lambda^2} \lambda_{SM} |H|^6
- \left(\frac{c_t}{\Lambda^2} y_t |H|^2 \bar{Q}_L H^c t_R + \frac{c_b}{\Lambda^2} y_b |H|^2 \bar{Q}_L H b_R + \frac{c_\tau}{\Lambda^2} y_\tau |H|^2 \bar{L}_L H \tau_R + \text{h.c.} \right)
+ \frac{\alpha_s c_g}{4\pi \Lambda^2} |H|^2 G_{\mu\nu}^a G_a^{\mu\nu} + \frac{\alpha' c_\gamma}{4\pi \Lambda^2} |H|^2 B_{\mu\nu} B^{\mu\nu}
+ \frac{ig c_{HW}}{16\pi^2 \Lambda^2} (D^{\mu} H)^{\dagger} \sigma_k (D^{\nu} H) W_{\mu\nu}^k + \frac{ig' c_{HB}}{16\pi^2 \Lambda^2} (D^{\mu} H)^{\dagger} (D^{\nu} H) B_{\mu\nu}
+ \frac{ig c_W}{2\Lambda^2} (H^{\dagger} \sigma_k \overleftrightarrow{D}^{\mu} H) D^{\nu} W_{\mu\nu}^k + \frac{ig' c_B}{2\Lambda^2} (H^{\dagger} \overleftrightarrow{D}^{\mu} H) \partial^{\nu} B_{\mu\nu}
+ \mathcal{L}_{CP} + \mathcal{L}_{4f},$$
(A.1)

where α_s is the strong coupling constant and $\alpha' \equiv g'^2/4\pi$.

The full set of D=6 operators that can be formed out of the SM field content was first obtained in [22] and reduced to a non-redundant minimal set in [23]. Here, we employed equations of motion to move to the basis used in [24, 160] and then imposed constraints from precision tests to neglect a class of operators whose effect is already constrained to be at most 1% with respect to the SM, following [161–165]. Including these operators would have a negligible numerical impact on the analysis, given the experimental and theoretical errors.

Precision measurements also lead to the approximate restrictions [24]

$$\frac{c_{HB}}{16\pi^2} = -\frac{c_{HW}}{16\pi^2} = -c_B = c_W \,, \tag{A.2}$$

which we will employ in the following. Thus our setup corresponds to a restricted strongly-interacting light Higgs (SILH) Lagrangian [166] where c_T has been set to zero and the relations (A.2) are used.

We note here that we do not include the effects of the chromomagnetic dipole operator, which has been shown be significant in processes such as $pp \to t\bar{t}$, $pp \to h$, $pp \to t\bar{t}h$, [167–169] as well as Higgs boson pair production [170]. Nevertheless, the chromomagnetic operator is subleading from the point of view of weakly interacting UV dynamics [171], and we therefore leave it to future work.

The terms contributing to multi-Higgs production via gluon fusion at the LHC at D=6 EFT are:

$$\mathcal{L}_{h^{n}} = -\mu^{2}|H|^{2} - \lambda|H|^{4} - \left(y_{t}\bar{Q}_{L}H^{c}t_{R} + y_{b}\bar{Q}_{L}Hb_{R} + \text{h.c.}\right)
+ \frac{c_{H}}{2\Lambda^{2}}(\partial^{\mu}|H|^{2})^{2} - \frac{c_{6}}{\Lambda^{2}}\lambda_{\text{SM}}|H|^{6} + \frac{\alpha_{s}c_{g}}{4\pi\Lambda^{2}}|H|^{2}G_{\mu\nu}^{a}G_{a}^{\mu\nu}
- \left(\frac{c_{t}}{\Lambda^{2}}y_{t}|H|^{2}\bar{Q}_{L}H^{c}t_{R} + \frac{c_{b}}{\Lambda^{2}}y_{b}|H|^{2}\bar{Q}_{L}Hb_{R} + \text{h.c.}\right),$$
(A.3)

where the first line includes the relevant Standard Model terms that will receive corrections from D=6 operators. For the purposes of the current study, we set $C_H=0$ in what follows. We also assume minimal flavour violation [172], which leads to the coefficients of the Yukawa-like terms in the last row of eq. (A.3) being proportional to the (SM-like) Yukawa couplings.

Examining the relevant terms in the scalar potential and expanding about the electroweak minimum, we get:

$$\mathcal{L}_{\text{self}} = -\mu^2 \frac{(v+h)^2}{2} - \lambda \frac{(v+h)^4}{4} - \frac{c_6 \lambda_{\text{SM}}}{\Lambda^2} \frac{(v+h)^6}{8}$$

$$= -\frac{\mu^2}{2} (v^2 + 2hv + h^2) - \frac{\lambda}{4} (v^4 + 4hv^3 + 6h^2v^2 + 4h^3v + h^4)$$

$$-\frac{c_6 \lambda_{\text{SM}}}{8\Lambda^2} (v^6 + 6v^5h + 15v^4h^2 + 20h^3v^3 + 15v^2h^4 + 6h^5v + h^6) . \tag{A.4}$$

Omitting terms with h^n , n > 4, and constant terms we arrive at

$$\mathcal{L}_{\text{self}} = -\frac{\mu^2}{2} (2hv + h^2) - \frac{\lambda}{4} (4hv^3 + 6h^2v^2 + 4h^3v + h^4) - \frac{c_6\lambda_{\text{SM}}}{8\Lambda^2} (6hv^5 + 15h^2v^4 + 20h^3v^3 + 15h^4v^2) + \dots$$
(A.5)

Finally, we focus on the fermion-Higgs boson interactions that receive contributions from

$$\mathcal{L}_{hf} = -\frac{y_f}{\sqrt{2}} \bar{f}_L(h+v) f_R - \frac{c_f y_f}{\Lambda^2} \frac{(v+h)^2}{2} \bar{f}_L \frac{(v+h)}{\sqrt{2}} f_R + \text{h.c.} , \qquad (A.6)$$

where $f = t, b, \ldots$, with $f_{L,R}$ the left- and right-handed fields, and the first term comes from the SM whereas the second term is a dimension-6 contribution. Expanding, we obtain

$$\mathcal{L}_{hf} = -\frac{y_f v}{\sqrt{2}} \left(1 + \frac{c_t v^2}{2\Lambda^2} \right) \bar{f}_L f_R - \frac{y_f}{\sqrt{2}} \left(1 + \frac{3c_f v^2}{2\Lambda^2} \right) \bar{f}_L f_R h$$
$$-\frac{y_f}{\sqrt{2}} \left(\frac{3c_f v}{2\Lambda^2} \right) \bar{f}_L f_R h^2 - \frac{y_f}{\sqrt{2}} \left(\frac{c_f}{2\Lambda^2} \right) \bar{f}_L f_R h^3 + \text{h.c.}. \tag{A.7}$$

The first line gives the expression for the modified fermion mass,

$$m_f = \frac{y_f v}{\sqrt{2}} \left(1 + \frac{c_t v^2}{2\Lambda^2} \right) , \tag{A.8}$$

and we can re-express eq. (A.7) in terms of this:

$$\mathcal{L}_{hf} = -m_f \bar{f}_L f_R - \frac{m_f}{v} \left(1 + \frac{c_f v^2}{\Lambda^2} \right) \bar{f}_L f_R h$$

$$- \frac{m_f}{v} \left(\frac{3c_f v}{2\Lambda^2} \right) \bar{f}_L f_R h^2 - \frac{m_f}{v} \left(\frac{c_f}{2\Lambda^2} \right) \bar{f}_L f_R h^3 + \text{h.c.}.$$
(A.9)

The final term that we need to consider is

$$\mathcal{L}_{hg} = \frac{\alpha_s c_g}{4\pi \Lambda^2} |H|^2 G_{\mu\nu}^a G_a^{\mu\nu}
= \frac{\alpha_s c_g}{4\pi \Lambda^2} \frac{(h+v)^2}{2} G_{\mu\nu}^a G_a^{\mu\nu}
= \frac{\alpha_s c_g}{4\pi \Lambda^2} (hv + \frac{h^2}{2}) G_{\mu\nu}^a G_a^{\mu\nu} + \dots ,$$
(A.10)

where the omitted constant term can be absorbed into an unobservable re-definition of the gluon wave function.

We thus obtain the following interactions in terms of the Higgs boson scalar h, relevant to Higgs boson multi-production:

$$\mathcal{L}_{D=6} = -\frac{m_h^2}{2v} (1 + c_6) h^3 - \frac{m_h^2}{8v^2} (1 + 6c_6) h^4 + \frac{\alpha_s c_g}{4\pi} \left(\frac{h}{v} + \frac{h^2}{2v^2} \right) G_{\mu\nu}^a G_a^{\mu\nu}$$

$$- \left[\frac{m_t}{v} (1 + c_t) \bar{t}_L t_R h + \frac{m_b}{v} (1 + c_b) \bar{b}_L b_R h + \text{h.c.} \right]$$

$$- \left[\frac{m_t}{v^2} \left(\frac{3c_t}{2} \right) \bar{t}_L t_R h^2 + \frac{m_b}{v^2} \left(\frac{3c_b}{2} \right) \bar{b}_L b_R h^2 + \text{h.c.} \right]$$

$$- \left[\frac{m_t}{v^3} \left(\frac{c_t}{2} \right) \bar{t}_L t_R h^3 + \frac{m_b}{v^3} \left(\frac{c_b}{2} \right) \bar{b}_L b_R h^3 + \text{h.c.} \right],$$
(A.11)

where we have explicitly written down the contributing components of the Q_L doublets.

B The electroweak chiral lagrangian including a light Higgs boson

The D=6 Lagrangian of eq. (A.3) represents a "linear" realization of an effective field theory, including the leading terms in terms of "canonical dimensions" D, and assuming baryon- and lepton-number conservation. This is also sometimes referred to as "SMEFT". An alternative way to organize the EFT is by chiral dimensions, which yields a "nonlinear" realization.

In this generalization of the SM, the gauge interactions are unchanged (at leading order), but general anomalous couplings are introduced for the physical Higgs boson. To do this in a consistent, gauge-invariant way, the scalar fields of the theory have to be decomposed into the three Goldstone fields φ^a , described by:

$$U = \exp(2i\varphi^a T^a/v) = \exp(2i\Phi/v), \qquad (B.1)$$

where

$$\Phi = \varphi^a T^a = \frac{1}{\sqrt{2}} \begin{pmatrix} \varphi^0 / \sqrt{2} & \varphi^+ \\ \varphi^- & -\varphi^0 / \sqrt{2} \end{pmatrix} , \qquad (B.2)$$

and where T^a are the generators of SU(2). The polar decomposition of the Higgs doublet H is then given by:

$$H = \frac{v+h}{\sqrt{2}}U\begin{pmatrix} 0\\1 \end{pmatrix} , \tag{B.3}$$

where h is the physical Higgs boson.

Under electroweak gauge transformations $SU(2)_L \times U(1)_Y$:

$$U \to g_L U g_Y^{\dagger} , \quad h \to h , \quad g_{L,R} \in \mathrm{SU}(2)_{L,R} ,$$
 (B.4)

such that the h is invariant, and its couplings can be consistently modified. The transofmrations g_L , and the U(1)_Y subgroup of g_R are gauged, so that the covariant derivatives are given by:⁷

$$D_{\mu}U = \partial_{\mu}U + igW_{\mu}U - ig'B_{\mu}UT_3 , \quad D_{\mu}h = \partial_{\mu}h . \tag{B.5}$$

⁷The term "nonlinear" describing this EFT comes from the fact that the scalar sector of the SM possesses a larger symmetry $SU_L \times SU_R$, known as the chiral electroweak symmetry, under which the Goldstone bosons φ^a transform nonlinearly, in contrast to the usual Higgs doublet field, which transforms linearly [159].

New dynamics may appear in the Higgs sector at a new physics scale $f \sim \mathcal{O}(\text{TeV})$. This could be, e.g. composite, pseudo-Goldstone Higgs particles [173–177], but also by other models with a modified Higgs sector with either weak or strong couplings. We can then parametrize deviations of the SM couplings by a quantity $\xi = v^2/f^2$, where $v = 246 \,\text{GeV}$ is the electroweak scale. Anomalous contributions, with respect to the SM, of order ξ in the Higgs couplings will generically lead to a cut-off $\Lambda = 4\pi f$ in the effective description of the new Higgs dynamics. This picture might be supplemented by TeV-scale (order f) new degrees of freedom (non-standard fermions, extra pseudo-Goldstone bosons), integrated out in the EFT at the electroweak scale v. The EFT can then be organized in full generality [178] as a double expansion in $\xi = v^2/f^2$ and $f^2/\Lambda^2 = 1/16\pi^2$, which are the two dimensionless parameters that can be formed out of the three relevant scales v, f and Λ . They are both small under the condition $v \ll f \ll \Lambda$. The expansion in ξ amounts to an expansion of the Lagrangian in operators of increasing canonical dimension. The expansion in f^2/Λ^2 , corresponds to a loop expansion or, equivalently, to an expansion in terms of increasing chiral dimension (χ) . To leading order in chiral dimensions, and to first order in ξ , the SM effective Lagrangian can be written in nonlinear notation as

$$\mathcal{L}_{2} = -\frac{1}{2} \langle G_{\mu\nu} G^{\mu\nu} \rangle - \frac{1}{2} \langle W_{\mu\nu} W^{\mu\nu} \rangle - \frac{1}{4} B_{\mu\nu} B^{\mu\nu} + \bar{q} i \mathcal{D} q + \bar{l} i \mathcal{D} l + \bar{u} i \mathcal{D} u + \bar{d} i \mathcal{D} d + \bar{e} i \mathcal{D} e
+ \frac{v^{2}}{4} \langle L_{\mu} L^{\mu} \rangle \left(1 + F_{U}(h) \right) + \frac{1}{2} \partial_{\mu} h \partial^{\mu} h - V(h)
- v \left[\bar{q} \left(Y_{u} + \sum_{n=1}^{3} Y_{u}^{(n)} \left(\frac{h}{v} \right)^{n} \right) U P_{+} r + \bar{q} \left(Y_{d} + \sum_{n=1}^{3} Y_{d}^{(n)} \left(\frac{h}{v} \right)^{n} \right) U P_{-} r
+ \bar{l} \left(Y_{e} + \sum_{n=1}^{3} Y_{e}^{(n)} \left(\frac{h}{v} \right)^{n} \right) U P_{-} \eta + \text{h.c.} \right] ,$$
(B.6)

with $L_{\mu} = iUD_{\mu}U^{\dagger}$, $P_{\pm} = 1/2 \pm T_3$, and

$$F_{U} = (2 - a_{2}) \frac{h}{v} + (1 - 2a_{2}) \left(\frac{h}{v}\right)^{2} - \frac{4}{3} a_{2} \left(\frac{h}{v}\right)^{3} - \frac{1}{3} a_{2} \left(\frac{h}{v}\right)^{4},$$

$$V = \frac{m_{h}^{2}}{2} h^{2} + \frac{m_{h}^{2} v^{2}}{2} \left[\left(1 + \frac{4}{3} a_{1} - \frac{3}{2} a_{2}\right) \left(\frac{h}{v}\right)^{3} + \left(\frac{1}{4} + 2a_{1} - \frac{25}{12} a_{2}\right) \left(\frac{h}{v}\right)^{4} + (a_{1} - a_{2}) \left(\frac{h}{v}\right)^{5} + \frac{a_{1} - a_{2}}{6} \left(\frac{h}{v}\right)^{6} \right],$$
(B.8)

$$Y_f^{(1)} = \left(1 - \frac{a_2}{2}\right)Y_f + 2\bar{Y}_f, \qquad Y_f^{(2)} = 3Y_f^{(3)} = -\frac{a_2}{2}Y_f + 3\bar{Y}_f, \qquad f = u, d, e.$$
 (B.9)

For generality, we have included generic flavor matrices \bar{Y}_f arising at NLO. In scenarios with minimal flavor violation [172], we can assume $\bar{Y}_f \propto Y_f$, as we did for the D=6 EFT (i.e. linear) scenario.

When applying the chiral Lagrangian formalism to processes that arise only at one-loop level in the SM, such as $h \to gg$, $h \to \gamma\gamma$ or $h \to Z\gamma$, terms at NLO (chiral dimension 4, or loop order 1) become relevant, in addition to loops with modified couplings from eq. (B.6). For the complete list of NLO operators we refer the reader to [34]. The relevant terms here are $\sim e^2 F_{\mu\nu} F^{\mu\nu} h$, $\sim eg' F_{\mu\nu} Z^{\mu\nu} h$ and $\sim g_s^2 \langle G_{\mu\nu} G^{\mu\nu} \rangle h$.

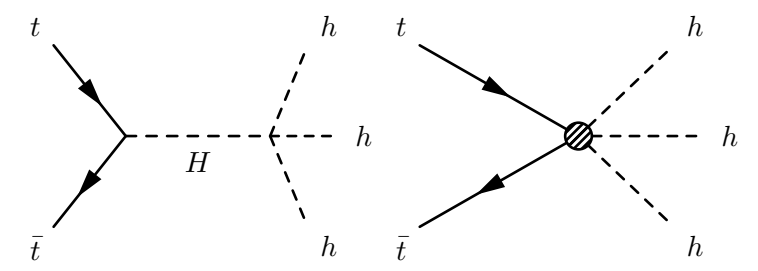


Figure 6. The $t\bar{t} \to hhh$ process used to validate the implementation of the $t\bar{t}hhh$ vertex. The process is shown in the model with a new heavy scalar (H) and in the limit of $M_H \gg \sqrt{\hat{s}}$.

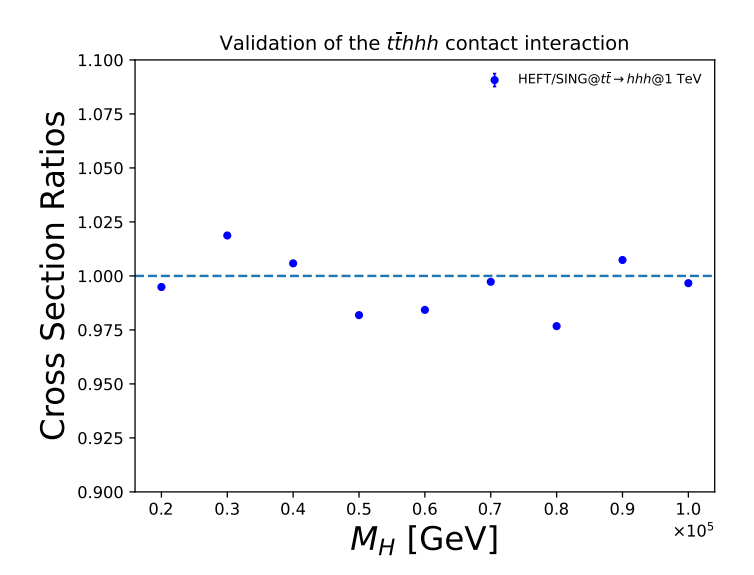


Figure 7. The ratio of cross sections between for $t\bar{t} \to hhh$ between the anomalous interaction (HEFT) and the heavy scalar (H) descriptions. See main text for further details.

In summary, the terms from the electroweak chiral Lagrangian relevant to multi-Higgs boson production, up to $gg \to hhh$, are given by [159, 179]:

$$\mathcal{L}_{\chi} \supset -c_{hhh}\lambda_{SM}vh^{3} - c_{hhhh}\frac{\lambda_{SM}}{4}h^{4} + \frac{\alpha_{s}}{8\pi} \left(c_{ggh}\frac{h}{v} + c_{gghh}\frac{h^{2}}{v^{2}}\right)G_{\mu\nu}^{a}G_{a}^{\mu\nu} \\
- \left[\frac{m_{t}}{v}c_{t}\bar{t}_{L}t_{R}h + \frac{m_{b}}{v}c_{b}\bar{b}_{L}b_{R}h + \text{h.c.}\right] \\
- \left[\frac{m_{t}}{v^{2}}c_{tt}\bar{t}_{L}t_{R}h^{2} + \frac{m_{b}}{v^{2}}c_{bb}\bar{b}_{L}b_{R}h^{2} + \text{h.c.}\right] \\
- \left[\frac{m_{t}}{v^{3}}\left(c_{ttt}\right)\bar{t}_{L}t_{R}h^{3} + \frac{m_{b}}{v^{3}}\left(c_{bbb}\right)\bar{b}_{L}b_{R}h^{3} + \text{h.c.}\right],$$
(B.10)

where we have again taken $\lambda_{\rm SM} \equiv m_h^2/2v^2$. The identifications that yield the phenomenological Lagrangian employed in this article, eq. (2.2), are: $c_{hhh} \rightarrow (1+c_3)$, $c_{hhhh} \rightarrow (1+d_4)$, $c_{ggh} \rightarrow 2c_{g1}/3$, $c_{gghh} \rightarrow c_{g2}/3$, $c_f \rightarrow (1+c_{f1})$, $c_{ff} \rightarrow c_{f2}$ and $c_{fff} \rightarrow c_{f3}/2$.

C Validation of the Monte Carlo implementation

Almost all vertices relevant in triple Higgs boson production are present in pair production. Therefore, these were validated using the HiggsPair model in HERWIG 7 Monte Carlo event

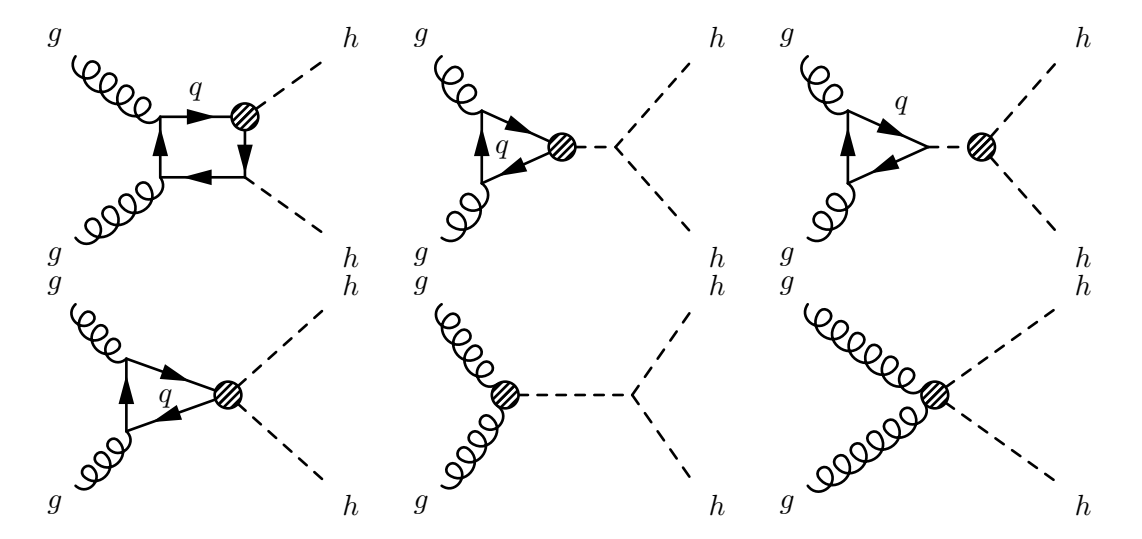


Figure 8. Example Feynman diagrams with *one* EFT operator insertion contributing to Higgs boson pair production.

	HL-LHC 3σ	HL-LHC 5σ	FCC-hh 3σ	FCC-hh 5σ
d_4	[-38.4, 36.0]	[-90.3, 81.0]	[-17.8, 20.8]	[-28.9, 23.2]
c_{t3}	[-2.8, 2.5]	[-6.4, 5.7]	[-0.5, 0.6]	[-0.9, 0.7]

Table 7. The 3σ evidence and 5σ discovery limits on for triple Higgs boson production with up to triple powers of anomalous operators at the matrix element-squared level, for the c_{t3} and d_4 coefficients at $13 \text{ TeV}/3000 \text{ fb}^{-1}$, and $100 \text{ TeV}/20 \text{ ab}^{-1}$, marginalized over c_{t2} , d_3 and either d_4 , or c_{t3} .

generator, with minor modifications, in the $gg \to hh$ process. Validation of the new tthhh contact interaction was performed by considering the processes $t\bar{t} \to hhh$ at 1 TeV in the $t\bar{t}$ center-of-mass frame without a PDF involved. The processes were calculated both in the HEFT and in a model with a heavy scalar (H) that couples to $t\bar{t}$ and hhh only. This implies taking the limit of the effective field theory directly and checking whether the effective vertex functions as expected. The matching of the coefficient of eq. (2.2) with the singlet model, e.g. of [18], implies that $c_{t3} = 2v^2/M_H^2$, when the quartic coupling between the heavy scalar and the three Higgs bosons is set to $\lambda_{1112} = 1$ and the mixing angle $\theta = \pi/2$ such that the SM Higgs boson is decoupled. Figure 7 shows the ratio of the anomalous $t\bar{t}hhh$ interaction cross section over the heavy scalar cross section for various masses of the heavy scalar, chosen to be much higher than the center-of-mass energy.

D Feynman diagrams

Figures 8 and 9 represent the Feynman diagrams for either one or two insertions of the operators used in the present article in Higgs boson pair production. Figures 10 and 11 represent the Feynman diagrams for either one or two insertions in the context of Higgs boson triple production.

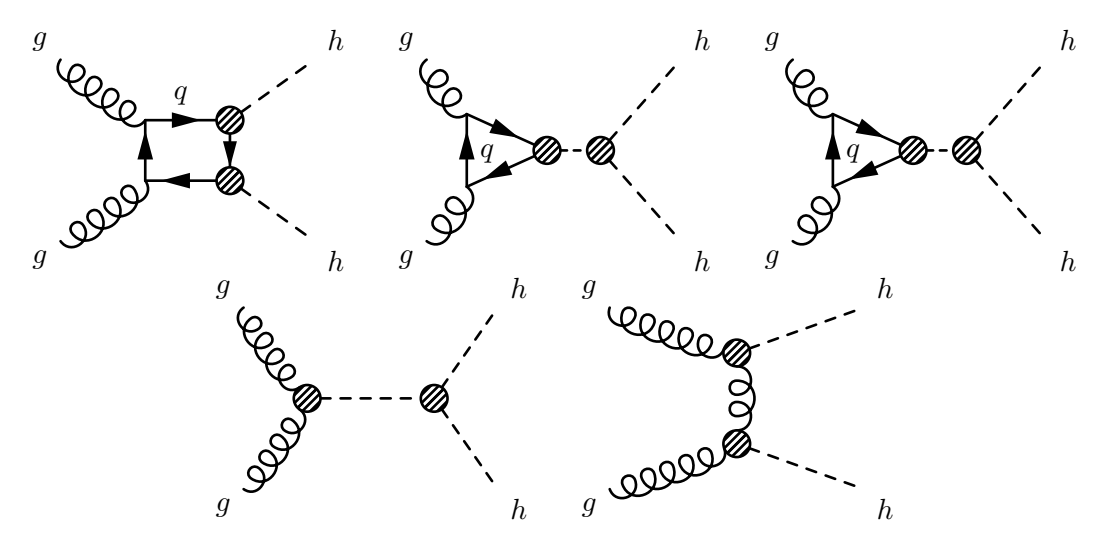


Figure 9. Example Feynman diagrams with *two* EFT operator insertions contributing to Higgs boson pair production.

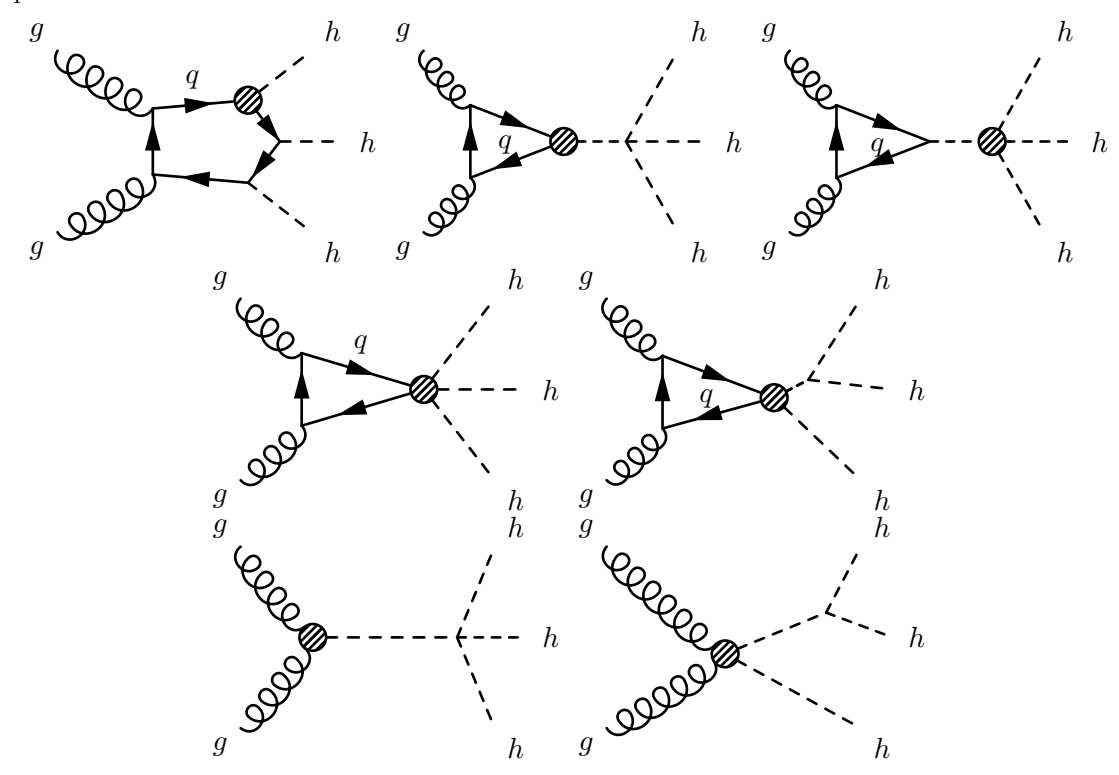


Figure 10. Example Feynman diagrams with *one* EFT operator insertion contributing to Higgs boson triple production.

	HL-LHC 68%	HL-LHC 95%	FCC-hh 68%	FCC-hh 95%
d_4	[-6.1, 9.7]	[-10.4, 16.1]	[-4.0, 9.6]	[-10.1, 19.6]
c_{t3}	[-0.5, 0.9]	[-1.0, 3.9]	[-0.1, 0.3]	[-0.7, 0.3]

Table 8. The 68% C.L. (1σ) and 95% C.L (2σ) limits on c_{t3} and d_4 for triple Higgs boson production with up to *triple powers* of anomalous operators at the matrix element-squared level, at $13 \text{ TeV}/3000 \text{ fb}^{-1}$, and $100 \text{ TeV}/20 \text{ ab}^{-1}$, marginalized over c_{t2} , d_3 and either d_4 , or c_{t3} .

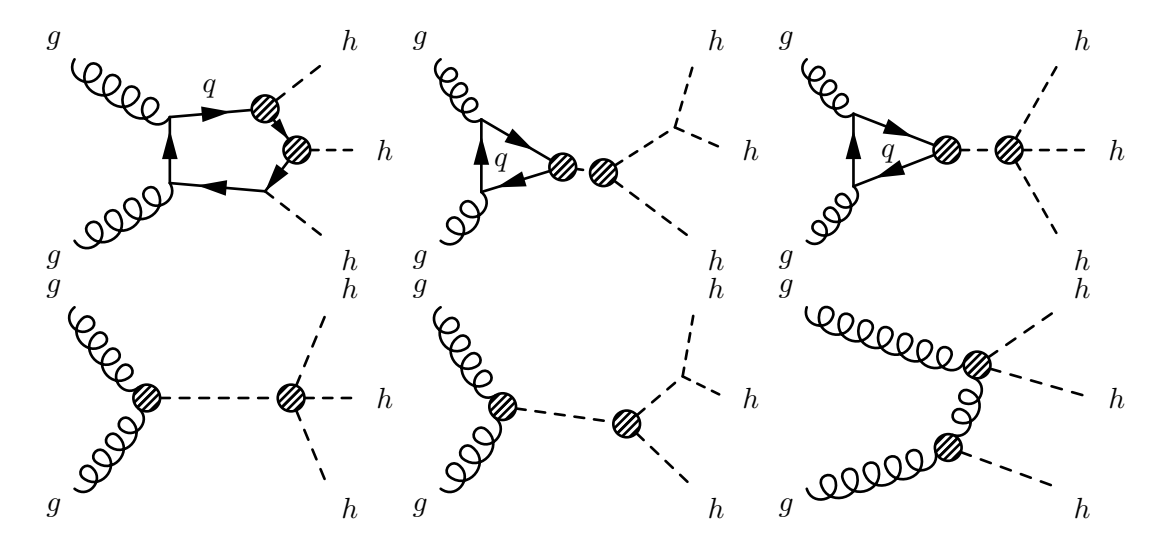


Figure 11. Example Feynman diagrams with *two* EFT operator insertions contributing to Higgs boson triple production.

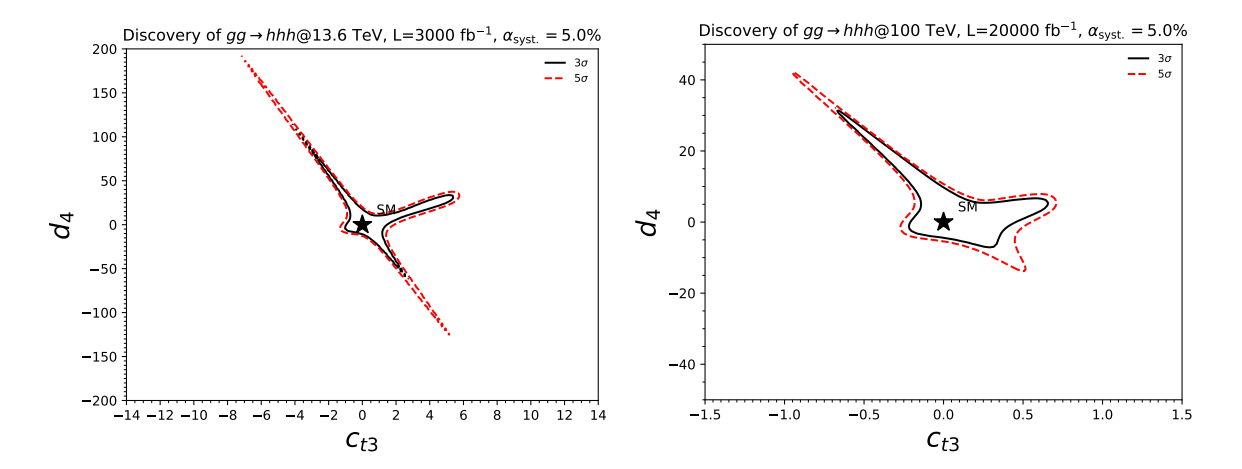


Figure 12. The 3σ evidence (black solid) and 5σ discovery (red dashed) curves on the (c_{t3}, d_4) -plane for triple Higgs boson production with up to *triple powers* of anomalous operators at the matrix element-squared level, at $13 \text{ TeV}/3000 \text{ fb}^{-1}$ (left), and $100 \text{ TeV}/20 \text{ ab}^{-1}$ (right), marginalized over the c_{t2} and d_3 anomalous couplings. Note the differences in the axes ranges at each collider.

E Discovery and limits with up to three powers of anomalous operators

We present here for completeness, the evidence/discovery boundaries and the 1σ and 2σ limits for the HL-LHC and FCC-hh, obtained with up to three powers of the anomalous operators at the matrix element-squared level. Since we are only considering the set $\{d_4, c_{t3}, d_3, c_{t2}\}$ in our phenomenological analysis, there can only be diagrams with up to two insertions, and the third power only comes from interference terms of these diagrams with single-insertion operators. This can be generated within MG5_aMC, by:

generate g g > h h h [noborn=MHEFT QCD] MHEFT^2<=3

Figures 12 and 13 are to be compared to figures 4 and 5, respectively, and tables 7 and 8 to tables 5 and 6, respectively. As can be clearly observed by examining the plots, as well as by

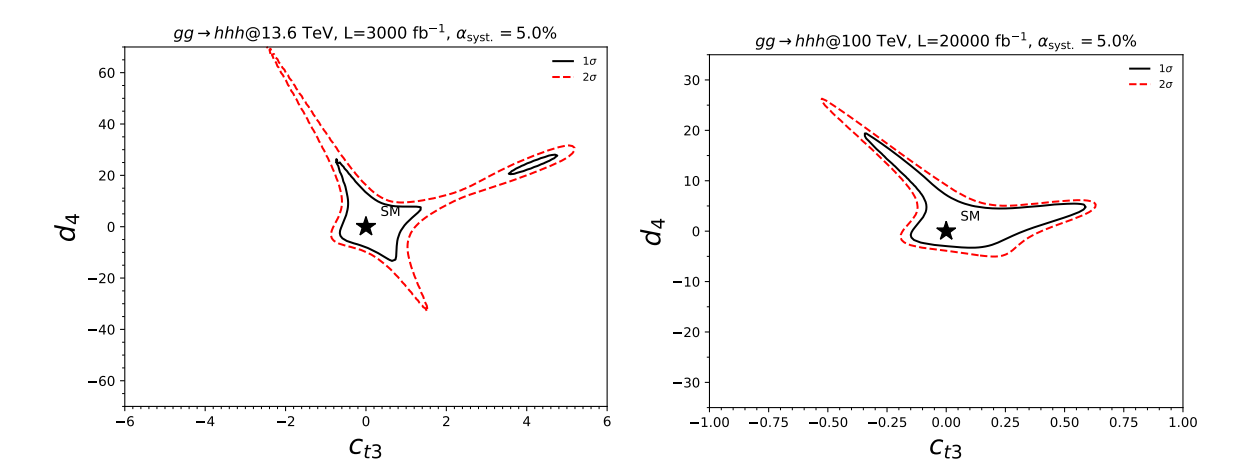


Figure 13. The 68% C.L. (1σ , black solid) and 95% C.L (2σ , red dashed) limit on the (c_{t3} , d_4)-plane for triple Higgs boson production with up to *triple powers* of anomalous operators at the matrix element-squared level, at $13 \text{ TeV}/3000 \text{ fb}^{-1}$ (left), and $100 \text{ TeV}/20 \text{ ab}^{-1}$ (right), marginalized over the c_{t2} and d_3 anomalous couplings. Note the differences in the axes ranges at each collider.

1	0.796	0.181	1					
d_3	-0.786	0.181		_				
c_{g1}	-0.386	0.0412	0.150					
c_{g2}	0.971	-0.123	-0.715	0.853				
c_{t1}	4.86	-1.87	-1.02	2.56	5.91			
c_{t2}	-5.57	1.70	2.08	-5.06	-13.9	10.0		
c_{b1}	-0.0900	-0.0656	0.224	-0.526	-0.298	1.17	0.0964	
c_{b2}	0.0629	0.0668	-0.199	0.468	0.224	-1.01	-0.174	0.0786
	1	d_3	c_{g1}	c_{g2}	c_{t1}	c_{t2}	c_{b1}	c_{b2}

Table 9. Polynomial coefficients, A_i (second column only) and B_{ij} , relevant for the determination of the cross section for leading-order Higgs boson pair production, in the form $\sigma/\sigma_{\rm SM} - 1 = \sum_i A_i c_i + \sum_{i,j} B_{ij} c_i c_j$, where $c_i \in \{d_3, c_{g1}, c_{g2}, c_{t1}, c_{t2}, c_{b1}, c_{b2}, \}$, at $E_{\rm CM} = 13.6$ TeV.

the one-dimensional quantitative limits in the tables, this treatment does not substantially alter either the expected evidence/discovery boundaries, or the limits.

F Cross section fits for triple and double Higgs boson production at various energies

This appendix provides the coefficients of the polynomial function for the cross section $\sigma/\sigma_{\rm SM}-1=\sum_i A_i c_i+\sum_{i,j} B_{ij} c_i c_j$, where $c_i\in\{d_3,d_4,c_{g1},c_{g2},c_{t1},c_{t2},c_{t3},c_{b1},c_{b2},c_{b3}\}$, for Higgs boson pair and production triple production. The coefficients for Higgs boson pair production for $E_{\rm CM}=13.6,\ 13,\ 14,\ 27,\ {\rm and}\ 100\, TeV$ are shown in tables 9, 10, 12, 14, 16, respectively, and for triple production in tables 1, 11, 13, 15, 17.

Open Access. This article is distributed under the terms of the Creative Commons Attribution License (CC-BY4.0), which permits any use, distribution and reproduction in any medium, provided the original author(s) and source are credited.

d_3	-0.846	0.179						
c_{g1}	-0.385	0.164	0.406					
c_{g2}	1.03	-0.438	-1.07	0.777				
c_{t1}	4.92	-2.08	-1.63	3.34	6.37			
c_{t2}	-5.85	2.48	3.09	-5.32	-16.2	11.2		
c_{b1}	-0.00554	0.00287	0.244	-0.289	-0.238	0.662	0.0400	
c_{b2}	-0.0117	0.00464	-0.138	0.159	0.101	-0.339	-0.0461	0.0133
	1	d_3	c_{g1}	c_{g2}	c_{t1}	c_{t2}	c_{b1}	c_{b2}

Table 10. Polynomial coefficients, A_i (second column only) and B_{ij} , relevant for the determination of the cross section for leading-order Higgs boson pair production, in the form $\sigma/\sigma_{\text{SM}} - 1 = \sum_i A_i c_i + \sum_{i,j} B_{ij} c_i c_j$, where $c_i \in \{d_3, c_{g1}, c_{g2}, c_{t1}, c_{t2}, c_{b1}, c_{b2}, \}$, at $E_{\text{CM}} = 13 \text{ TeV}$.

d_3	-0.824	0.225									
d_4	-0.147	-0.0640	0.0755								
c_{g1}	-0.229	0.123	-0.0151	0.0168							
c_{g2}	1.35	-0.609	-0.0411	-0.168	0.470						
c_{t1}	6.76	-3.22	-0.00692	-0.888	4.78	12.3					
c_{t2}	-3.82	3.24	-1.59	0.864	-3.37	-19.5	16.1				
c_{t3}	-2.76	-0.384	1.92	-0.0730	-1.16	-3.36	-17.6	12.4			
c_{b1}	-0.121	0.167	-0.123	0.0440	-0.137	-0.871	2.00	-1.45	0.0661		
c_{b2}	0.0382	-0.0607	0.0478	-0.0159	0.0470	0.306	-0.748	0.566	-0.0501	0.00950	
c_{b3}	0.0676	-0.0445	0.0137	-0.0120	0.0535	0.294	-0.378	0.135	-0.0217	0.00804	0.00239
	1	d_3	d_4	c_{g1}	c_{g2}	c_{t1}	c_{t2}	c_{t3}	c_{b1}	c_{b2}	c_{b3}

Table 11. Polynomial coefficients, A_i (second column only) and B_{ij} , relevant for the determination of the cross section for leading-order Higgs boson triple production, in the form $\sigma/\sigma_{\rm SM}-1=\sum_i A_i c_i+\sum_{i,j}B_{ij}c_ic_j$, where $c_i\in\{d_3,c_{g1},c_{g2},c_{t1},c_{t2},c_{b1},c_{b2},\}$, at $E_{\rm CM}=13$ TeV.

d_3	-0.857	0.282						
c_{g1}	-0.386	0.291	0.0772					
c_{g2}	0.957	-1.08	-0.613	1.38				
c_{t1}	5.00	-2.38	-1.12	3.20	6.39			
c_{t2}	-5.86	3.50	1.76	-6.17	-15.8	11.0		
c_{b1}	-0.0500	0.165	0.101	-0.514	-0.298	0.865	0.0529	
c_{b2}	-0.00429	-0.0655	-0.0420	0.228	0.0704	-0.324	-0.0489	0.0115
	1	d_3	c_{g1}	c_{g2}	c_{t1}	c_{t2}	c_{b1}	c_{b2}

Table 12. Polynomial coefficients, A_i (second column only) and B_{ij} , relevant for the determination of the cross section for leading-order Higgs boson pair production, in the form $\sigma/\sigma_{\text{SM}} - 1 = \sum_i A_i c_i + \sum_{i,j} B_{ij} c_i c_j$, where $c_i \in \{d_3, c_{g1}, c_{g2}, c_{t1}, c_{t2}, c_{b1}, c_{b2}, \}$, at $E_{\text{CM}} = 14$ TeV.

d_3	-0.827	0.414									
d_4	-0.211	-0.110	0.0511								
c_{g1}	-0.208	0.210	-0.0282	0.0265							
c_{g2}	1.28	-0.700	-0.0655	-0.177	0.440						
c_{t1}	6.67	-3.57	-0.372	-0.901	4.55	11.8					
c_{t2}	-3.73	4.96	-0.993	1.26	-3.59	-18.2	15.5				
c_{t3}	-2.67	-2.19	1.61	-0.558	-0.551	-3.38	-18.1	12.9			
c_{b1}	-0.0693	0.187	-0.0567	0.0473	-0.0998	-0.496	1.24	-0.974	0.0268		
c_{b2}	0.0853	0.136	-0.0783	0.0346	-0.00548	-0.00213	1.04	-1.27	0.0525	0.0319	
c_{b3}	0.0827	0.00135	-0.0231	0.000427	0.0404	0.216	0.0953	-0.350	0.00865	0.0160	0.00300
	1	d_3	d_4	c_{g1}	c_{g2}	c_{t1}	c_{t2}	c_{t3}	c_{b1}	c_{b2}	c_{b3}

Table 13. Polynomial coefficients, A_i (second column only) and B_{ij} , relevant for the determination of the cross section for leading-order Higgs boson triple production, in the form $\sigma/\sigma_{\rm SM} - 1 = \sum_i A_i c_i + \sum_{i,j} B_{ij} c_i c_j$, where $c_i \in \{d_3, c_{g1}, c_{g2}, c_{t1}, c_{t2}, c_{b1}, c_{b2}, \}$, at $E_{\rm CM} = 14$ TeV.

d_3	-0.690	0.643						
c_{g1}	-0.393	-0.0942	0.0638					
c_{g2}	0.828	-1.23	0.0452	0.600		_		
c_{t1}	4.62	-3.54	-0.482	3.67	7.15		_	
c_{t2}	-5.66	3.00	0.882	-3.29	-15.0	8.52		
c_{b1}	0.0110	0.186	-0.0437	-0.167	-0.327	0.159	0.0172	
c_{b2}	-0.0117	-0.126	0.0307	0.113	0.214	-0.0967	-0.0236	0.00807
	1	d_3	c_{g1}	c_{g2}	c_{t1}	c_{t2}	c_{b1}	c_{b2}

Table 14. Polynomial coefficients, A_i (second column only) and B_{ij} , relevant for the determination of the cross section for leading-order Higgs boson pair production, in the form $\sigma/\sigma_{\rm SM}-1=\sum_i A_i c_i+\sum_{i,j} B_{ij} c_i c_j$, where $c_i \in \{d_3, c_{g1}, c_{g2}, c_{t1}, c_{t2}, c_{b1}, c_{b2}, \}$, at $E_{\rm CM}=27$ TeV.

d_3	-0.675	0.193									
d_4	-0.124	-0.113	0.0795								
c_{g1}	-0.388	0.198	-0.0413	0.0516							
c_{g2}	1.25	-0.696	0.191	-0.358	0.628						
c_{t1}	7.00	-2.82	0.0138	-1.55	5.17	12.9					
c_{t2}	-3.88	3.35	-1.75	1.61	-5.96	-19.5	16.9				
c_{t3}	-3.62	-0.745	2.15	-0.129	1.15	-7.00	-18.4	15.5			
c_{b1}	0.0800	0.0750	-0.105	0.0275	-0.127	-0.0145	1.16	-1.41	0.0345		
c_{b2}	0.0412	-0.0807	0.0628	-0.0362	0.142	0.337	-0.941	0.756	-0.0414	0.0145	
c_{b3}	0.0562	-0.0116	-0.0107	-0.00778	0.0224	0.176	-0.0138	-0.194	0.00701	-0.00196	0.000963
	1	d_3	d_4	c_{g1}	c_{g2}	c_{t1}	c_{t2}	c_{t3}	c_{b1}	c_{b2}	c_{b3}

Table 15. Polynomial coefficients, A_i (second column only) and B_{ij} , relevant for the determination of the cross section for leading-order Higgs boson triple production, in the form $\sigma/\sigma_{\rm SM}-1=\sum_i A_i c_i+\sum_{i,j} B_{ij} c_i c_j$, where $c_i \in \{d_3, c_{g1}, c_{g2}, c_{t1}, c_{t2}, c_{b1}, c_{b2}, \}$, at $E_{\rm CM}=27$ TeV.

d_3	-0.644	0.105						
c_{g1}	-0.276	0.0790	0.0322					
c_{g2}	0.644	-0.0898	-0.406	2.01				
c_{t1}	4.60	-1.44	-0.753	2.91	5.55			
c_{t2}	-5.75	1.74	1.08	-5.34	-14.5	9.86		
c_{b1}	-0.0759	0.0174	0.0295	-0.253	-0.260	0.427	0.00829	
c_{b2}	0.0391	0.0119	-0.0714	0.805	0.387	-0.839	-0.0490	0.0830
	1	d_3	c_{g1}	c_{g2}	c_{t1}	c_{t2}	c_{b1}	c_{b2}

Table 16. Polynomial coefficients, A_i (second column only) and B_{ij} , relevant for the determination of the cross section for leading-order Higgs boson pair production, in the form $\sigma/\sigma_{\text{SM}} - 1 = \sum_i A_i c_i + \sum_{i,j} B_{ij} c_i c_j$, where $c_i \in \{d_3, c_{g1}, c_{g2}, c_{t1}, c_{t2}, c_{b1}, c_{b2}, \}$, at $E_{\text{CM}} = 100 \text{ TeV}$.

d_3	-0.643	0.185									
d_4	-0.175	-0.0386	0.0352								
c_{g1}	-0.236	0.0972	0.00817	0.0153							
c_{g2}	1.29	-0.811	0.119	-0.204	0.898						
c_{t1}	6.43	-2.46	-0.331	-0.810	5.10	10.8					
c_{t2}	-3.93	3.10	-0.724	0.704	-7.00	-17.1	14.2				
c_{t3}	-4.64	-1.26	2.01	0.186	3.73	-8.21	-21.9	28.6			
c_{b1}	-0.0679	0.0514	-0.0113	0.0119	-0.116	-0.290	0.466	-0.342	0.00383		
c_{b2}	0.0750	-0.0144	-0.0122	-0.00757	0.0246	0.217	-0.0383	-0.338	-0.000788	0.00169	
c_{b3}	-0.0157	0.0642	-0.0330	0.00962	-0.154	-0.195	0.697	-0.962	0.0113	0.00292	0.0108
	1	d_3	d_4	c_{g1}	c_{g2}	c_{t1}	c_{t2}	c_{t3}	c_{b1}	c_{b2}	c_{b3}

Table 17. Polynomial coefficients, A_i (second column only) and B_{ij} , relevant for the determination of the cross section for leading-order Higgs boson triple production, in the form $\sigma/\sigma_{\rm SM} - 1 = \sum_i A_i c_i + \sum_{i,j} B_{ij} c_i c_j$, where $c_i \in \{d_3, c_{g1}, c_{g2}, c_{t1}, c_{t2}, c_{b1}, c_{b2}, \}$, at $E_{\rm CM} = 100$ TeV.

References

- [1] A. Papaefstathiou, G. Tetlalmatzi-Xolocotzi and A. Tonero, *Triple Higgs Boson Production in a Higgs Effective Theory*, https://gitlab.com/apapaefs/multihiggs_loop_sm, (2023).
- [2] P.W. Higgs, Broken Symmetries and the Masses of Gauge Bosons, Phys. Rev. Lett. 13 (1964) 508 [INSPIRE].
- [3] F. Englert and R. Brout, Broken Symmetry and the Mass of Gauge Vector Mesons, Phys. Rev. Lett. 13 (1964) 321 [INSPIRE].
- [4] G.S. Guralnik, C.R. Hagen and T.W.B. Kibble, Global Conservation Laws and Massless Particles, Phys. Rev. Lett. 13 (1964) 585 [INSPIRE].
- [5] ATLAS collaboration, Observation of a new particle in the search for the Standard Model Higgs boson with the ATLAS detector at the LHC, Phys. Lett. B 716 (2012) 1 [arXiv:1207.7214] [INSPIRE].
- [6] CMS collaboration, Observation of a New Boson at a Mass of 125 GeV with the CMS Experiment at the LHC, Phys. Lett. B 716 (2012) 30 [arXiv:1207.7235] [INSPIRE].
- [7] G.C. Dorsch, S.J. Huber and J.M. No, A strong electroweak phase transition in the 2HDM after LHC8, JHEP 10 (2013) 029 [arXiv:1305.6610] [INSPIRE].

- [8] J.M. No and M. Ramsey-Musolf, Probing the Higgs Portal at the LHC Through Resonant di-Higgs Production, Phys. Rev. D 89 (2014) 095031 [arXiv:1310.6035] [INSPIRE].
- [9] D. Curtin, P. Meade and C.-T. Yu, Testing Electroweak Baryogenesis with Future Colliders, JHEP 11 (2014) 127 [arXiv:1409.0005] [INSPIRE].
- [10] S. Profumo, M.J. Ramsey-Musolf, C.L. Wainwright and P. Winslow, Singlet-catalyzed electroweak phase transitions and precision Higgs boson studies, Phys. Rev. D 91 (2015) 035018 [arXiv:1407.5342] [INSPIRE].
- [11] G.A. White, A Pedagogical Introduction to Electroweak Baryogenesis [DOI:10.1088/978-1-6817-4457-5] [INSPIRE].
- [12] P. Basler et al., Strong First Order Electroweak Phase Transition in the CP-Conserving 2HDM Revisited, JHEP 02 (2017) 121 [arXiv:1612.04086] [INSPIRE].
- [13] J. Bernon, L. Bian and Y. Jiang, A new insight into the phase transition in the early Universe with two Higgs doublets, JHEP 05 (2018) 151 [arXiv:1712.08430] [INSPIRE].
- [14] G. Kurup and M. Perelstein, Dynamics of Electroweak Phase Transition In Singlet-Scalar Extension of the Standard Model, Phys. Rev. D 96 (2017) 015036 [arXiv:1704.03381] [INSPIRE].
- [15] G.C. Dorsch, S.J. Huber, K. Mimasu and J.M. No, The Higgs Vacuum Uplifted: Revisiting the Electroweak Phase Transition with a Second Higgs Doublet, JHEP 12 (2017) 086 [arXiv:1705.09186] [INSPIRE].
- [16] M.J. Ramsey-Musolf, The electroweak phase transition: a collider target, JHEP **09** (2020) 179 [arXiv:1912.07189] [INSPIRE].
- [17] H.-L. Li, M. Ramsey-Musolf and S. Willocq, Probing a scalar singlet-catalyzed electroweak phase transition with resonant di-Higgs boson production in the 4b channel, Phys. Rev. D 100 (2019) 075035 [arXiv:1906.05289] [INSPIRE].
- [18] A. Papaefstathiou and G. White, The electro-weak phase transition at colliders: confronting theoretical uncertainties and complementary channels, JHEP 05 (2021) 099 [arXiv:2010.00597] [INSPIRE].
- [19] A. Papaefstathiou and G. White, *The Electro-Weak Phase Transition at Colliders: Discovery Post-Mortem*, *JHEP* **02** (2022) 185 [arXiv:2108.11394] [INSPIRE].
- [20] A. Papaefstathiou, T. Robens and G. White, Signal strength and W-boson mass measurements as a probe of the electro-weak phase transition at colliders Snowmass White Paper, in the proceedings of the Snowmass 2021, Seattle, U.S.A., July 17–26 (2022) [arXiv:2205.14379] [INSPIRE].
- [21] J. Zuk, C. Balazs, A. Papaefstathiou and G. White, The effective potential in Fermi gauges beyond the standard model, Eur. Phys. J. C 84 (2024) 66 [arXiv:2212.04046] [INSPIRE].
- [22] W. Buchmuller and D. Wyler, Effective Lagrangian Analysis of New Interactions and Flavor Conservation, Nucl. Phys. B 268 (1986) 621 [INSPIRE].
- [23] B. Grzadkowski, M. Iskrzynski, M. Misiak and J. Rosiek, Dimension-Six Terms in the Standard Model Lagrangian, JHEP 10 (2010) 085 [arXiv:1008.4884] [INSPIRE].
- [24] J. Elias-Miro, J.R. Espinosa, E. Masso and A. Pomarol, Higgs windows to new physics through d = 6 operators: constraints and one-loop anomalous dimensions, JHEP 11 (2013) 066 [arXiv:1308.1879] [INSPIRE].

- [25] F. Feruglio, The chiral approach to the electroweak interactions, Int. J. Mod. Phys. A 8 (1993) 4937 [hep-ph/9301281] [INSPIRE].
- [26] J. Bagger et al., The strongly interacting W W system: Gold plated modes, Phys. Rev. D 49 (1994) 1246 [hep-ph/9306256] [INSPIRE].
- [27] V. Koulovassilopoulos and R.S. Chivukula, The phenomenology of a nonstandard Higgs boson in W(L) W(L) scattering, Phys. Rev. D 50 (1994) 3218 [hep-ph/9312317] [INSPIRE].
- [28] C.P. Burgess, J. Matias and M. Pospelov, A Higgs or not a Higgs? What to do if you discover a new scalar particle, Int. J. Mod. Phys. A 17 (2002) 1841 [hep-ph/9912459] [INSPIRE].
- [29] L.-M. Wang and Q. Wang, Nonstandard Higgs in electroweak chiral Lagrangian, hep-ph/0605104 [INSPIRE].
- [30] B. Grinstein and M. Trott, A Higgs-Higgs bound state due to new physics at a TeV, Phys. Rev. D 76 (2007) 073002 [arXiv:0704.1505] [INSPIRE].
- [31] R. Alonso et al., The Effective Chiral Lagrangian for a Light Dynamical "Higgs Particle", Phys. Lett. B 722 (2013) 330 [Erratum ibid. 726 (2013) 926] [arXiv:1212.3305] [INSPIRE].
- [32] G. Buchalla, O. Catá and C. Krause, On the Power Counting in Effective Field Theories, Phys. Lett. B 731 (2014) 80 [arXiv:1312.5624] [INSPIRE].
- [33] G. Buchalla and O. Cata, Effective Theory of a Dynamically Broken Electroweak Standard Model at NLO, JHEP 07 (2012) 101 [arXiv:1203.6510] [INSPIRE].
- [34] G. Buchalla, O. Catà and C. Krause, Complete Electroweak Chiral Lagrangian with a Light Higgs at NLO, Nucl. Phys. B 880 (2014) 552 [arXiv:1307.5017] [INSPIRE].
- [35] G. Buchalla et al., Complete One-Loop Renormalization of the Higgs-Electroweak Chiral Lagrangian, Nucl. Phys. B 928 (2018) 93 [arXiv:1710.06412] [INSPIRE].
- [36] CMS collaboration, Search for Higgs boson pair production in the $bb\tau\tau$ final state in proton-proton collisions at $\sqrt(s) = 8$ TeV, Phys. Rev. D **96** (2017) 072004 [arXiv:1707.00350] [INSPIRE].
- [37] CMS collaboration, Search for Higgs boson pair production in events with two bottom quarks and two tau leptons in proton-proton collisions at \sqrt{s} =13TeV, Phys. Lett. B 778 (2018) 101 [arXiv:1707.02909] [INSPIRE].
- [38] CMS collaboration, Search for resonant and nonresonant Higgs boson pair production in the $b\bar{b}\ell\nu\ell\nu$ final state in proton-proton collisions at $\sqrt{s}=13$ TeV, JHEP **01** (2018) 054 [arXiv:1708.04188] [INSPIRE].
- [39] CMS collaboration, Search for Higgs boson pair production in the $\gamma\gamma b\bar{b}$ final state in pp collisions at $\sqrt{s} = 13$ TeV, Phys. Lett. B 788 (2019) 7 [arXiv:1806.00408] [INSPIRE].
- [40] CMS collaboration, Search for production of Higgs boson pairs in the four b quark final state using large-area jets in proton-proton collisions at $\sqrt{s} = 13$ TeV, JHEP **01** (2019) 040 [arXiv:1808.01473] [INSPIRE].
- [41] CMS collaboration, Search for nonresonant Higgs boson pair production in the bbbb final state at $\sqrt{s} = 13$ TeV, JHEP **04** (2019) 112 [arXiv:1810.11854] [INSPIRE].
- [42] CMS collaboration, Combination of searches for Higgs boson pair production in proton-proton collisions at $\sqrt{s} = 13$ TeV, Phys. Rev. Lett. 122 (2019) 121803 [arXiv:1811.09689] [INSPIRE].
- [43] CMS collaboration, Search for nonresonant Higgs boson pair production in final states with two bottom quarks and two photons in proton-proton collisions at $\sqrt{s} = 13$ TeV, JHEP **03** (2021) 257 [arXiv:2011.12373] [INSPIRE].

- [44] CMS collaboration, Search for Higgs Boson Pair Production in the Four b Quark Final State in Proton-Proton Collisions at s=13 TeV, Phys. Rev. Lett. 129 (2022) 081802 [arXiv:2202.09617] [INSPIRE].
- [45] CMS collaboration, Search for nonresonant Higgs boson pair production in final state with two bottom quarks and two tau leptons in proton-proton collisions at s=13 TeV, Phys. Lett. B 842 (2023) 137531 [arXiv:2206.09401] [INSPIRE].
- [46] CMS collaboration, Search for Higgs boson pairs decaying to WW*WW*, WW* $\tau\tau$, and $\tau\tau\tau\tau$ in proton-proton collisions at $\sqrt{s} = 13$ TeV, JHEP 07 (2023) 095 [arXiv:2206.10268] [INSPIRE].
- [47] CMS collaboration, Search for nonresonant Higgs boson pair production in the four leptons plus twob jets final state in proton-proton collisions at $\sqrt{s} = 13$ TeV, JHEP **06** (2023) 130 [arXiv:2206.10657] [INSPIRE].
- [48] ATLAS collaboration, Search For Higgs Boson Pair Production in the $\gamma\gamma b\bar{b}$ Final State using pp Collision Data at $\sqrt{s}=8$ TeV from the ATLAS Detector, Phys. Rev. Lett. 114 (2015) 081802 [arXiv:1406.5053] [INSPIRE].
- [49] ATLAS collaboration, Search for Higgs boson pair production in the $b\bar{b}b\bar{b}$ final state from pp collisions at $\sqrt{s}=8$ TeVwith the ATLAS detector, Eur. Phys. J. C **75** (2015) 412 [arXiv:1506.00285] [INSPIRE].
- [50] ATLAS collaboration, Searches for Higgs boson pair production in the $hh \rightarrow bb\tau\tau, \gamma\gamma WW^*, \gamma\gamma bb, bbbb$ channels with the ATLAS detector, Phys. Rev. D **92** (2015) 092004 [arXiv:1509.04670] [INSPIRE].
- [51] ATLAS collaboration, Search for pair production of Higgs bosons in the bbbb final state using proton-proton collisions at $\sqrt{s} = 13$ TeV with the ATLAS detector, Phys. Rev. D **94** (2016) 052002 [arXiv:1606.04782] [INSPIRE].
- [52] ATLAS collaboration, Search for pair production of Higgs bosons in the bbbb final state using proton-proton collisions at $\sqrt{s} = 13$ TeV with the ATLAS detector, JHEP **01** (2019) 030 [arXiv:1804.06174] [INSPIRE].
- [53] ATLAS collaboration, Search for Higgs boson pair production in the $\gamma\gamma b\bar{b}$ final state with 13 TeV pp collision data collected by the ATLAS experiment, JHEP 11 (2018) 040 [arXiv:1807.04873] [INSPIRE].
- [54] ATLAS collaboration, Search for Higgs boson pair production in the $\gamma\gamma WW^*$ channel using pp collision data recorded at $\sqrt{s}=13$ TeV with the ATLAS detector, Eur. Phys. J. C 78 (2018) 1007 [arXiv:1807.08567] [INSPIRE].
- [55] ATLAS collaboration, Search for resonant and non-resonant Higgs boson pair production in the $b\bar{b}\tau^+\tau^-$ decay channel in pp collisions at $\sqrt{s}=13$ TeV with the ATLAS detector, Phys. Rev. Lett. 121 (2018) 191801 [Erratum ibid. 122 (2019) 089901] [arXiv:1808.00336] [INSPIRE].
- [56] ATLAS collaboration, Search for Higgs boson pair production in the $b\bar{b}WW^*$ decay mode at $\sqrt{s} = 13$ TeV with the ATLAS detector, JHEP **04** (2019) 092 [arXiv:1811.04671] [INSPIRE].
- [57] ATLAS collaboration, Search for Higgs boson pair production in the $WW^{(*)}WW^{(*)}$ decay channel using ATLAS data recorded at $\sqrt{s}=13$ TeV, JHEP **05** (2019) 124 [arXiv:1811.11028] [INSPIRE].
- [58] ATLAS collaboration, Combination of searches for Higgs boson pairs in pp collisions at $\sqrt{s} = 13$ TeV with the ATLAS detector, Phys. Lett. B 800 (2020) 135103 [arXiv:1906.02025] [INSPIRE].

- [59] ATLAS collaboration, Search for non-resonant Higgs boson pair production in the bbl $\nu\ell\nu$ final state with the ATLAS detector in pp collisions at $\sqrt{s} = 13$ TeV, Phys. Lett. B 801 (2020) 135145 [arXiv:1908.06765] [INSPIRE].
- [60] ATLAS collaboration, Search for the $HH \to b\bar{b}b\bar{b}$ process via vector-boson fusion production using proton-proton collisions at $\sqrt{s} = 13$ TeV with the ATLAS detector, JHEP **07** (2020) 108 [Erratum ibid. **01** (2021) 145] [arXiv:2001.05178] [INSPIRE].
- [61] ATLAS collaboration, Search for Higgs boson pair production in the two bottom quarks plus two photons final state in pp collisions at $\sqrt{s} = 13$ TeV with the ATLAS detector, Phys. Rev. D 106 (2022) 052001 [arXiv:2112.11876] [INSPIRE].
- [62] ATLAS collaboration, Search for resonant and non-resonant Higgs boson pair production in the $b\bar{b}\tau^+\tau^-$ decay channel using 13 TeV pp collision data from the ATLAS detector, JHEP **07** (2023) 040 [arXiv:2209.10910] [INSPIRE].
- [63] ATLAS collaboration, Constraints on the Higgs boson self-coupling from single- and double-Higgs production with the ATLAS detector using pp collisions at s=13 TeV, Phys. Lett. B 843 (2023) 137745 [arXiv:2211.01216] [INSPIRE].
- [64] ATLAS collaboration, Search for nonresonant pair production of Higgs bosons in the bb bb final state in pp collisions at s=13 TeV with the ATLAS detector, Phys. Rev. D 108 (2023) 052003 [arXiv:2301.03212] [INSPIRE].
- [65] ATLAS collaboration, Studies of new Higgs boson interactions through nonresonant HH production in the $b\bar{b}\gamma\gamma$ final state in pp collisions at $\sqrt{s}=13$ TeV with the ATLAS detector, JHEP **01** (2024) 066 [arXiv:2310.12301] [INSPIRE].
- [66] U. Baur, T. Plehn and D.L. Rainwater, Measuring the Higgs Boson Self Coupling at the LHC and Finite Top Mass Matrix Elements, Phys. Rev. Lett. 89 (2002) 151801 [hep-ph/0206024] [INSPIRE].
- [67] U. Baur, T. Plehn and D.L. Rainwater, Determining the Higgs Boson Selfcoupling at Hadron Colliders, Phys. Rev. D 67 (2003) 033003 [hep-ph/0211224] [INSPIRE].
- [68] U. Baur, T. Plehn and D.L. Rainwater, Probing the Higgs selfcoupling at hadron colliders using rare decays, Phys. Rev. D 69 (2004) 053004 [hep-ph/0310056] [INSPIRE].
- [69] M.J. Dolan, C. Englert and M. Spannowsky, New Physics in LHC Higgs boson pair production, Phys. Rev. D 87 (2013) 055002 [arXiv:1210.8166] [INSPIRE].
- [70] A. Papaefstathiou, L.L. Yang and J. Zurita, Higgs boson pair production at the LHC in the $b\bar{b}W^+W^-$ channel, Phys. Rev. D 87 (2013) 011301 [arXiv:1209.1489] [INSPIRE].
- [71] J. Cao et al., Pair Production of a 125 GeV Higgs Boson in MSSM and NMSSM at the LHC, JHEP 04 (2013) 134 [arXiv:1301.6437] [INSPIRE].
- [72] F. Goertz, A. Papaefstathiou, L.L. Yang and J. Zurita, *Higgs Boson self-coupling measurements using ratios of cross sections*, *JHEP* **06** (2013) 016 [arXiv:1301.3492] [INSPIRE].
- [73] A. Arbey, M. Battaglia and F. Mahmoudi, Supersymmetric Heavy Higgs Bosons at the LHC, Phys. Rev. D 88 (2013) 015007 [arXiv:1303.7450] [INSPIRE].
- [74] D. de Florian and J. Mazzitelli, Two-loop virtual corrections to Higgs pair production, Phys. Lett. B 724 (2013) 306 [arXiv:1305.5206] [INSPIRE].
- [75] R.S. Gupta, H. Rzehak and J.D. Wells, How well do we need to measure the Higgs boson mass and self-coupling?, Phys. Rev. D 88 (2013) 055024 [arXiv:1305.6397] [INSPIRE].

- [76] U. Ellwanger, Higgs pair production in the NMSSM at the LHC, JHEP 08 (2013) 077 [arXiv:1306.5541] [INSPIRE].
- [77] A.J. Barr, M.J. Dolan, C. Englert and M. Spannowsky, Di-Higgs final states augMT2ed selecting hh events at the high luminosity LHC, Phys. Lett. B 728 (2014) 308 [arXiv:1309.6318] [INSPIRE].
- [78] P. Maierhöfer and A. Papaefstathiou, *Higgs Boson pair production merged to one jet*, *JHEP* 03 (2014) 126 [arXiv:1401.0007] [INSPIRE].
- [79] D. de Florian and J. Mazzitelli, Higgs Boson Pair Production at Next-to-Next-to-Leading Order in QCD, Phys. Rev. Lett. 111 (2013) 201801 [arXiv:1309.6594] [INSPIRE].
- [80] M.J. Dolan, C. Englert, N. Greiner and M. Spannowsky, Further on up the road: hhjj production at the LHC, Phys. Rev. Lett. 112 (2014) 101802 [arXiv:1310.1084] [INSPIRE].
- [81] F. Goertz, A. Papaefstathiou, L.L. Yang and J. Zurita, Measuring the Higgs boson self-coupling at the LHC using ratios of cross sections, in the proceedings of the 25th Rencontres de Blois on Particle Physics and Cosmology, Blois, France, May 26–31 (2013) [arXiv:1309.3805] [INSPIRE].
- [82] R. Frederix et al., Higgs pair production at the LHC with NLO and parton-shower effects, Phys. Lett. B 732 (2014) 142 [arXiv:1401.7340] [INSPIRE].
- [83] J. Baglio, O. Eberhardt, U. Nierste and M. Wiebusch, Benchmarks for Higgs Pair Production and Heavy Higgs boson Searches in the Two-Higgs-Doublet Model of Type II, Phys. Rev. D 90 (2014) 015008 [arXiv:1403.1264] [INSPIRE].
- [84] D.E. Ferreira de Lima, A. Papaefstathiou and M. Spannowsky, Standard model Higgs boson pair production in the $(b\bar{b})(b\bar{b})$ final state, JHEP **08** (2014) 030 [arXiv:1404.7139] [INSPIRE].
- [85] D. de Florian and J. Mazzitelli, Next-to-Next-to-Leading Order QCD Corrections to Higgs Boson Pair Production, PoS LL2014 (2014) 029 [arXiv:1405.4704] [INSPIRE].
- [86] B. Hespel, D. Lopez-Val and E. Vryonidou, *Higgs pair production via gluon fusion in the Two-Higgs-Doublet Model*, *JHEP* **09** (2014) 124 [arXiv:1407.0281] [INSPIRE].
- [87] V. Barger et al., New physics in resonant production of Higgs boson pairs, Phys. Rev. Lett. 114 (2015) 011801 [arXiv:1408.0003] [INSPIRE].
- [88] S.I. Godunov, M.I. Vysotsky and E.V. Zhemchugov, Double Higgs production at LHC, see-saw type II and Georgi-Machacek model, J. Exp. Theor. Phys. 120 (2015) 369 [arXiv:1408.0184] [INSPIRE].
- [89] N. Liu, S. Hu, B. Yang and J. Han, Impact of top-Higgs couplings on Di-Higgs production at future colliders, JHEP 01 (2015) 008 [arXiv:1408.4191] [INSPIRE].
- [90] F. Maltoni, E. Vryonidou and M. Zaro, Top-quark mass effects in double and triple Higgs production in gluon-gluon fusion at NLO, JHEP 11 (2014) 079 [arXiv:1408.6542] [INSPIRE].
- [91] C.-Y. Chen, S. Dawson and I.M. Lewis, Exploring resonant di-Higgs boson production in the Higgs singlet model, Phys. Rev. D 91 (2015) 035015 [arXiv:1410.5488] [INSPIRE].
- [92] A.J. Barr et al., Higgs Self-Coupling Measurements at a 100 TeV Hadron Collider, JHEP 02 (2015) 016 [arXiv:1412.7154] [INSPIRE].
- [93] V. Martín Lozano, J.M. Moreno and C.B. Park, Resonant Higgs boson pair production in the $hh \to b\bar{b} \ WW \to b\bar{b}\ell^+\nu\ell^-\bar{\nu}$ decay channel, JHEP **08** (2015) 004 [arXiv:1501.03799] [INSPIRE].
- [94] A. Papaefstathiou, Discovering Higgs boson pair production through rare final states at a 100 TeV collider, Phys. Rev. D 91 (2015) 113016 [arXiv:1504.04621] [INSPIRE].

- [95] S. Dawson, A. Ismail and I. Low, What's in the loop? The anatomy of double Higgs production, Phys. Rev. D 91 (2015) 115008 [arXiv:1504.05596] [INSPIRE].
- [96] A.V. Kotwal, S. Chekanov and M. Low, Double Higgs Boson Production in the 4τ Channel from Resonances in Longitudinal Vector Boson Scattering at a 100 TeV Collider, Phys. Rev. D 91 (2015) 114018 [arXiv:1504.08042] [INSPIRE].
- [97] C.-T. Lu, J. Chang, K. Cheung and J.S. Lee, An exploratory study of Higgs-boson pair production, JHEP 08 (2015) 133 [arXiv:1505.00957] [INSPIRE].
- [98] A. Carvalho et al., Higgs Pair Production: Choosing Benchmarks With Cluster Analysis, JHEP 04 (2016) 126 [arXiv:1507.02245] [INSPIRE].
- [99] Q.-H. Cao, Y. Liu and B. Yan, Measuring trilinear Higgs coupling in WHH and ZHH productions at the high-luminosity LHC, Phys. Rev. D 95 (2017) 073006 [arXiv:1511.03311] [INSPIRE].
- [100] B. Batell, M. McCullough, D. Stolarski and C.B. Verhaaren, Putting a Stop to di-Higgs Modifications, JHEP 09 (2015) 216 [arXiv:1508.01208] [INSPIRE].
- [101] S. Dawson and I.M. Lewis, *NLO corrections to double Higgs boson production in the Higgs singlet model*, *Phys. Rev. D* **92** (2015) 094023 [arXiv:1508.05397] [INSPIRE].
- [102] Q.-H. Cao, B. Yan, D.-M. Zhang and H. Zhang, Resolving the Degeneracy in Single Higgs Production with Higgs Pair Production, Phys. Lett. B 752 (2016) 285 [arXiv:1508.06512] [INSPIRE].
- [103] S. Kanemura et al., Single and double production of the Higgs boson at hadron and lepton colliders in minimal composite Higgs models, Phys. Rev. D 94 (2016) 015028
 [arXiv:1603.05588] [INSPIRE].
- [104] R. Contino et al., Physics at a 100 TeV pp collider: Higgs and EW symmetry breaking studies, arXiv:1606.09408 [DOI:10.23731/CYRM-2017-003.255] [INSPIRE].
- [105] Q.-H. Cao et al., Double Higgs production at the 14 TeV LHC and a 100 TeV pp collider, Phys. Rev. D 96 (2017) 095031 [arXiv:1611.09336] [INSPIRE].
- [106] S. Banerjee, B. Batell and M. Spannowsky, Invisible decays in Higgs boson pair production, Phys. Rev. D 95 (2017) 035009 [arXiv:1608.08601] [INSPIRE].
- [107] T. Huang et al., Resonant di-Higgs boson production in the bbWW channel: Probing the electroweak phase transition at the LHC, Phys. Rev. D 96 (2017) 035007 [arXiv:1701.04442] [INSPIRE].
- [108] K. Nakamura et al., Di-higgs enhancement by neutral scalar as probe of new colored sector, Eur. Phys. J. C 77 (2017) 273 [arXiv:1701.06137] [INSPIRE].
- [109] I.M. Lewis and M. Sullivan, Benchmarks for Double Higgs Production in the Singlet Extended Standard Model at the LHC, Phys. Rev. D 96 (2017) 035037 [arXiv:1701.08774] [INSPIRE].
- [110] L. Di Luzio, R. Gröber and M. Spannowsky, Maxi-sizing the trilinear Higgs self-coupling: how large could it be?, Eur. Phys. J. C 77 (2017) 788 [arXiv:1704.02311] [INSPIRE].
- [111] R. Grober, M. Muhlleitner and M. Spira, Higgs Pair Production at NLO QCD for CP-violating Higgs Sectors, Nucl. Phys. B 925 (2017) 1 [arXiv:1705.05314] [INSPIRE].
- [112] J. Zurita, Di-Higgs production at the LHC and beyond, in the proceedings of the 5th Large Hadron Collider Physics Conference, Shanghai, China, May 15–20 (2017) [arXiv:1708.00892] [INSPIRE].

- [113] E. Arganda et al., Search strategies for pair production of heavy Higgs bosons decaying invisibly at the LHC, Nucl. Phys. B 929 (2018) 171 [arXiv:1710.07254] [INSPIRE].
- [114] A. Adhikary et al., Revisiting the non-resonant Higgs pair production at the HL-LHC, JHEP 07 (2018) 116 [arXiv:1712.05346] [INSPIRE].
- [115] M. Bauer, M. Carena and A. Carmona, Higgs Pair Production as a Signal of Enhanced Yukawa Couplings, Phys. Rev. Lett. 121 (2018) 021801 [arXiv:1801.00363] [INSPIRE].
- [116] F. Maltoni, D. Pagani and X. Zhao, Constraining the Higgs self-couplings at e^+e^- colliders, JHEP 07 (2018) 087 [arXiv:1802.07616] [INSPIRE].
- [117] S. Borowka et al., Probing the scalar potential via double Higgs boson production at hadron colliders, JHEP 04 (2019) 016 [arXiv:1811.12366] [INSPIRE].
- [118] D. Gonçalves et al., Higgs boson pair production at future hadron colliders: From kinematics to dynamics, Phys. Rev. D 97 (2018) 113004 [arXiv:1802.04319] [INSPIRE].
- [119] J. Chang et al., Higgs-boson-pair production H(→bb⁻)H(→ γγ) from gluon fusion at the HL-LHC and HL-100 TeV hadron collider, Phys. Rev. D 100 (2019) 096001 [arXiv:1804.07130] [INSPIRE].
- [120] P. Basler, S. Dawson, C. Englert and M. Mühlleitner, Showcasing HH production: Benchmarks for the LHC and HL-LHC, Phys. Rev. D 99 (2019) 055048 [arXiv:1812.03542] [INSPIRE].
- [121] A. Adhikary, S. Banerjee, R. Kumar Barman and B. Bhattacherjee, Resonant heavy Higgs searches at the HL-LHC, JHEP 09 (2019) 068 [arXiv:1812.05640] [INSPIRE].
- [122] J. Alison et al., Higgs boson potential at colliders: Status and perspectives, Rev. Phys. 5 (2020) 100045 [arXiv:1910.00012] [INSPIRE].
- [123] G. Li, L.-X. Xu, B. Yan and C.-P. Yuan, Resolving the degeneracy in top quark Yukawa coupling with Higgs pair production, Phys. Lett. B 800 (2020) 135070 [arXiv:1904.12006] [INSPIRE].
- [124] K. Cheung et al., Disentangling new physics effects on nonresonant Higgs boson pair production from gluon fusion, Phys. Rev. D 103 (2021) 015019 [arXiv:2003.11043] [INSPIRE].
- [125] T. Plehn and M. Rauch, The quartic higgs coupling at hadron colliders, Phys. Rev. D 72 (2005) 053008 [hep-ph/0507321] [INSPIRE].
- [126] A. Papaefstathiou and K. Sakurai, Triple Higgs boson production at a 100 TeV proton-proton collider, JHEP 02 (2016) 006 [arXiv:1508.06524] [INSPIRE].
- [127] C.-Y. Chen et al., Probing triple-Higgs productions via 4b2γ decay channel at a 100 TeV hadron collider, Phys. Rev. D 93 (2016) 013007 [arXiv:1510.04013] [INSPIRE].
- [128] B. Fuks, J.H. Kim and S.J. Lee, Probing Higgs self-interactions in proton-proton collisions at a center-of-mass energy of 100 TeV, Phys. Rev. D 93 (2016) 035026 [arXiv:1510.07697] [INSPIRE].
- [129] A. Papaefstathiou, Multi-Higgs Boson Production and Self-coupling Measurements at Hadron Colliders, Acta Phys. Polon. B 48 (2017) 1133 [INSPIRE].
- [130] B. Fuks, J.H. Kim and S.J. Lee, Scrutinizing the Higgs quartic coupling at a future 100 TeV proton-proton collider with taus and b-jets, Phys. Lett. B 771 (2017) 354 [arXiv:1704.04298] [INSPIRE].
- [131] T. Liu, K.-F. Lyu, J. Ren and H.X. Zhu, Probing the quartic Higgs boson self-interaction, Phys. Rev. D 98 (2018) 093004 [arXiv:1803.04359] [INSPIRE].

- [132] A. Papaefstathiou, G. Tetlalmatzi-Xolocotzi and M. Zaro, Triple Higgs boson production to six b-jets at a 100 TeV proton collider, Eur. Phys. J. C 79 (2019) 947 [arXiv:1909.09166] [INSPIRE].
- [133] D. de Florian, I. Fabre and J. Mazzitelli, Triple Higgs production at hadron colliders at NNLO in QCD, JHEP 03 (2020) 155 [arXiv:1912.02760] [INSPIRE].
- [134] M. Chiesa et al., Measuring the quartic Higgs self-coupling at a multi-TeV muon collider, JHEP 09 (2020) 098 [arXiv:2003.13628] [INSPIRE].
- [135] M. Abdughani et al., Probing the triple Higgs boson coupling with machine learning at the LHC, Phys. Rev. D 104 (2021) 056003 [arXiv:2005.11086] [INSPIRE].
- [136] A. Papaefstathiou, T. Robens and G. Tetlalmatzi-Xolocotzi, Triple Higgs Boson Production at the Large Hadron Collider with Two Real Singlet Scalars, JHEP 05 (2021) 193 [arXiv:2101.00037] [INSPIRE].
- [137] P. Stylianou and G. Weiglein, Constraints on the trilinear and quartic Higgs couplings from triple Higgs production at the LHC and beyond, Eur. Phys. J. C 84 (2024) 366 [arXiv:2312.04646] [INSPIRE].
- [138] C. Degrande et al., Automated one-loop computations in the standard model effective field theory, Phys. Rev. D 103 (2021) 096024 [arXiv:2008.11743] [INSPIRE].
- [139] F. Goertz, A. Papaefstathiou, L.L. Yang and J. Zurita, Higgs boson pair production in the D=6 extension of the SM, JHEP 04 (2015) 167 [arXiv:1410.3471] [INSPIRE].
- [140] A. Azatov, R. Contino, G. Panico and M. Son, Effective field theory analysis of double Higgs boson production via gluon fusion, Phys. Rev. D 92 (2015) 035001 [arXiv:1502.00539] [INSPIRE].
- [141] J. Alwall et al., MadGraph 5: Going Beyond, JHEP 06 (2011) 128 [arXiv:1106.0522] [INSPIRE].
- [142] V. Hirschi and O. Mattelaer, Automated event generation for loop-induced processes, JHEP 10 (2015) 146 [arXiv:1507.00020] [INSPIRE].
- [143] V. Hirschi, Computing the interference of loop-induced diagrams with a tree-level background with MadEvent in MG5_aMC, https://cp3.irmp.ucl.ac.be/projects/madgraph/wiki/LoopInducedTimesTree, (2016).
- [144] S. Bailey et al., Parton distributions from LHC, HERA, Tevatron and fixed target data: MSHT20 PDFs, Eur. Phys. J. C 81 (2021) 341 [arXiv:2012.04684] [INSPIRE].
- [145] J. de Blas et al., Higgs Boson Studies at Future Particle Colliders, JHEP **01** (2020) 139 [arXiv:1905.03764] [INSPIRE].
- [146] M. Bahr et al., Herwig++ Physics and Manual, Eur. Phys. J. C 58 (2008) 639 [arXiv:0803.0883] [INSPIRE].
- [147] S. Gieseke et al., Herwig++ 2.5 $Release\ Note,\ arXiv:1102.1672\ [INSPIRE].$
- [148] K. Arnold et al., Herwig++ 2.6 Release Note, arXiv:1205.4902 [INSPIRE].
- [149] J. Bellm et al., Herwig++ 2.7 Release Note, arXiv:1310.6877 [INSPIRE].
- [150] J. Bellm et al., Herwig 7.0/Herwig++ 3.0 release note, Eur. Phys. J. C 76 (2016) 196 [arXiv:1512.01178] [INSPIRE].
- [151] J. Bellm et al., Herwig 7.1 Release Note, arXiv:1705.06919 [INSPIRE].

- [152] J. Bellm et al., Herwig 7.2 release note, Eur. Phys. J. C 80 (2020) 452 [arXiv:1912.06509] [INSPIRE].
- [153] G. Bewick et al., Herwig 7.3 Release Note, arXiv:2312.05175 [INSPIRE].
- [154] A. Papaefstathiou, The HwSim analysis package for HERWIG 7, https://gitlab.com/apapaefs/hwsim.
- [155] ATLAS collaboration, Jet energy scale and resolution measured in proton-proton collisions at $\sqrt{s} = 13$ TeV with the ATLAS detector, Eur. Phys. J. C 81 (2021) 689 [arXiv:2007.02645] [INSPIRE].
- [156] <CMS collaboration, Jet energy scale and resolution measurement with Run 2 Legacy Data Collected by CMS at 13 TeV. https://cds.cern.ch/record/2792322 (2021).
- [157] HDECAY collaboration, eHDECAY: an Implementation of the Higgs Effective Lagrangian into HDECAY, Comput. Phys. Commun. 185 (2014) 3412 [arXiv:1403.3381] [INSPIRE].
- [158] CERN, Yellow Report webpage, https://twiki.cern.ch/twiki/bin/view/LHCPhysics/CERNYellowReportPageBR, (2016).
- [159] LHC HIGGS CROSS SECTION WORKING GROUP collaboration, Handbook of LHC Higgs Cross Sections: 4. Deciphering the Nature of the Higgs Sector, arXiv:1610.07922 [DOI:10.23731/CYRM-2017-002] [INSPIRE].
- [160] A. Pomarol and F. Riva, Towards the Ultimate SM Fit to Close in on Higgs Physics, JHEP 01 (2014) 151 [arXiv:1308.2803] [INSPIRE].
- [161] B. Dumont, S. Fichet and G. von Gersdorff, A Bayesian view of the Higgs sector with higher dimensional operators, JHEP 07 (2013) 065 [arXiv:1304.3369] [INSPIRE].
- [162] T. Corbett, O.J.P. Eboli, J. Gonzalez-Fraile and M.C. Gonzalez-Garcia, *Constraining anomalous Higgs interactions*, *Phys. Rev. D* **86** (2012) 075013 [arXiv:1207.1344] [INSPIRE].
- [163] T. Corbett, O.J.P. Eboli, J. Gonzalez-Fraile and M.C. Gonzalez-Garcia, Robust Determination of the Higgs Couplings: Power to the Data, Phys. Rev. D 87 (2013) 015022 [arXiv:1211.4580] [INSPIRE].
- [164] T. Corbett, O.J.P. Éboli, J. Gonzalez-Fraile and M.C. Gonzalez-Garcia, Determining Triple Gauge Boson Couplings from Higgs Data, Phys. Rev. Lett. 111 (2013) 011801 [arXiv:1304.1151] [INSPIRE].
- [165] R. Contino et al., Effective Lagrangian for a light Higgs-like scalar, JHEP 07 (2013) 035 [arXiv:1303.3876] [INSPIRE].
- [166] G.F. Giudice, C. Grojean, A. Pomarol and R. Rattazzi, The Strongly-Interacting Light Higgs, JHEP 06 (2007) 045 [hep-ph/0703164] [INSPIRE].
- [167] F. Maltoni, E. Vryonidou and C. Zhang, Higgs production in association with a top-antitop pair in the Standard Model Effective Field Theory at NLO in QCD, JHEP 10 (2016) 123 [arXiv:1607.05330] [INSPIRE].
- [168] N. Deutschmann, C. Duhr, F. Maltoni and E. Vryonidou, Gluon-fusion Higgs production in the Standard Model Effective Field Theory, JHEP 12 (2017) 063 [Erratum ibid. 02 (2018) 159] [arXiv:1708.00460] [INSPIRE].
- [169] S. Di Noi et al., γ5 schemes and the interplay of SMEFT operators in the Higgs-gluon coupling, Phys. Rev. D 109 (2024) 095024 [arXiv:2310.18221] [INSPIRE].

- [170] G. Heinrich and J. Lang, Combining chromomagnetic and four-fermion operators with leading SMEFT operators for gg → hh at NLO QCD, JHEP **05** (2024) 121 [arXiv:2311.15004] [INSPIRE].
- [171] R. Gröber et al., Effective Field Theory descriptions of Higgs boson pair production, LHCHWG-2022-004, CERN, Geneva (2022).
- [172] G. D'Ambrosio, G.F. Giudice, G. Isidori and A. Strumia, *Minimal flavor violation: An effective field theory approach*, *Nucl. Phys. B* **645** (2002) 155 [hep-ph/0207036] [INSPIRE].
- [173] K. Agashe, R. Contino and A. Pomarol, *The Minimal composite Higgs model*, *Nucl. Phys. B* **719** (2005) 165 [hep-ph/0412089] [INSPIRE].
- [174] R. Contino, L. Da Rold and A. Pomarol, Light custodians in natural composite Higgs models, Phys. Rev. D 75 (2007) 055014 [hep-ph/0612048] [INSPIRE].
- [175] R. Contino, The Higgs as a Composite Nambu-Goldstone Boson, in the proceedings of the Theoretical Advanced Study Institute in Elementary Particle Physics: Physics of the Large and the Small, Boulder, U.S.A., June 01–26 (2009) [DOI:10.1142/9789814327183_0005] [arXiv:1005.4269] [INSPIRE].
- [176] A. Falkowski, Pseudo-goldstone Higgs production via gluon fusion, Phys. Rev. D 77 (2008) 055018 [arXiv:0711.0828] [INSPIRE].
- [177] M. Carena, L. Da Rold and E. Pontón, Minimal Composite Higgs Models at the LHC, JHEP 06 (2014) 159 [arXiv:1402.2987] [INSPIRE].
- [178] G. Buchalla, O. Cata and C. Krause, A Systematic Approach to the SILH Lagrangian, Nucl. Phys. B 894 (2015) 602 [arXiv:1412.6356] [INSPIRE].
- [179] G. Buchalla et al., Higgs boson pair production in non-linear Effective Field Theory with full m_t -dependence at NLO QCD, JHEP **09** (2018) 057 [arXiv:1806.05162] [INSPIRE].